Improving Broader Sharing to Address Geographic Inequity in Liver Transplantation

Shubham Akshat
The Robert H. Smith School of Business, University of Maryland, College Park, MD 20742, sakshat@umd.edu

Liye Ma
The Robert H. Smith School of Business, University of Maryland, College Park, MD 20742, liyema@umd.edu

S. Raghavan
The Robert H. Smith School of Business and Institute for Systems Research
University of Maryland, College Park, MD 20742, raghavan@umd.edu

Problem definition: This paper studies the deceased-donor liver allocation policies in the United States (U.S.). In the transplant community, broader organ sharing is believed to mitigate geographic inequity in organ access, and recent policies are moving in that direction in principle. The liver allocation policy has gone through three major modifications in the last nine years. Despite these modifications, geographic inequity persists.

Methodology/results: In this study, we develop a patient's dynamic choice model to analyze her strategic response to a policy change. First, we study the impact of the Share 35 policy, a variant of broader sharing introduced in 2013, on the behavioral change of patients at the transplant centers (i.e., change in their organ acceptance probability), geographic equity, and efficiency (transplant quality, offer refusals, survival benefit from a transplant, and organ travel distance). We find that sicker patients became more selective in accepting organs (acceptance probability decreased) under the Share 35 policy. Second, we study the current Acuity Circles policy and conclude that it would result in lower efficiency (more offer refusals and a lower transplant benefit) than the previous Share 35 policy. Finally, we show that broader sharing in its current form may not be the best strategy to balance geographic equity and efficiency. The intuition is that by indiscriminately enlarging the pool of supply locations from where patients can receive offers, they tend to become more selective, resulting in more offer rejections and less efficiency. We illustrate that a policy that equalizes the supply (deceased donors)-to-demand (waiting list patients) ratios across geographies is better than Acuity Circles in achieving geographic equity at the lowest trade-off on efficiency metrics.

Managerial implications: The key message to policymakers is that they should move away from the 'one-size-fits-all' approach and focus on matching supply and demand to develop organ allocation policies that score well in terms of efficiency and geographic equity.

Key words: liver allocation, healthcare policy, geographic disparity, structural estimation, dynamic optimization

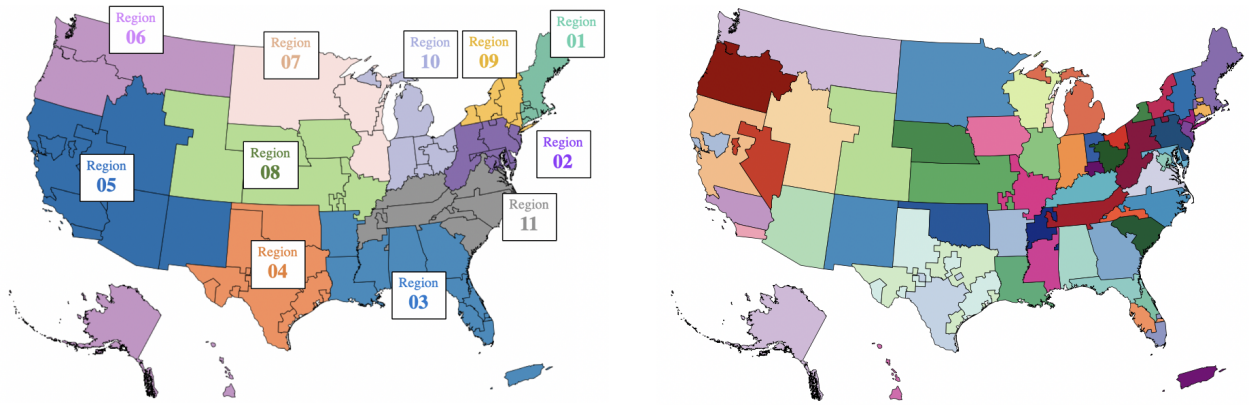

Figure 1 **The U.S. divided into 11 regions (left) comprising 58 DSAs (right).**

1. Introduction

In the United States (U.S.), an average of three people die every day waiting for a liver transplant, resulting in 1,133 lives lost in 2021. While 13,439 patients were added to the waiting list in 2021, only 9,236 patients received liver transplants. Liver transplantation is the only treatment option for patients with end-stage liver disease when other medical therapies have failed. Deceased donations have contributed to greater than 95% of liver donations in the last 15 years in the U.S. Unlike living donations, which can be arranged privately by a patient-donor pair, deceased-donor organs are considered *national* resources by law. The U.S. is divided into 11 geographic regions (Figure 1), consisting of 58 Donation Service Areas (DSAs). A DSA-based allocation policy had been in place for thirty years (from 1989 to Feb. 4, 2020) but was recently replaced by the Acuity Circles policy (Section 2.2). Medical urgency, used to rank patients for an organ offer, is quantitatively measured by the Model for End-Stage Liver Disease (MELD) score. The Pediatric End-Stage Liver Disease (PELD) severity score, a measure calculated slightly differently, is used for patients ≤ 12 years old. The MELD score reflects the probability of death within three months and ranges from 6 to 40, with a higher score indicating a greater mortality risk (Freeman et al. 2002). More serious patients are assigned Status 1A (for adults) and 1B (for non-adults); their number is fewer than 50 nationwide at any time.

The U.S. government created the Organ Procurement and Transplantation Network (OPTN) in 1984 to coordinate a nationwide transplant system and optimize the use of limited donor organs for transplants. Since 1986, the United Network for Organ Sharing (UNOS), a nonprofit private organization, has overseen the operations of OPTN. A key regulatory framework guiding organ transplantation is the 'Final Rule', which was adopted in 1998 by the Department of Health and Human Services (HHS) to establish a more detailed framework for the structure and operations of OPTN (HHS 1998). The Final Rule states that policies shall not be based on the candidate's place

Candidate UNOS status at transplant	Number functioning (Alive)	Survival rate
MELD/PELD 6-14	760	89.8
MELD/PELD 15-29	12549	90.2
MELD/PELD 30-34	3495	89.3
MELD/PELD ≥35	5286	87.0
Status 1A	934	83.8
Status 1B	377	89.0

Table 1 One year Kaplan-Meier graft survival rate based on 2012-2015 transplants. Follow-up done till December 18, 2020.

of residence or place of listing (a patient lists herself at the transplant center and joins the waiting list), except to the extent mandated by the other requirements of the Rule. The HHS (1998) [§121.8 (a), (b) and (c)] emphasizes equitable (with reducing inter-geographical variation in the transplant rates, patient survival rates, and waiting time as illustrative goals) and efficient allocation of organs (with avoiding wastage, and making the best use of donated organs as illustrative goals) as its policy development and performance goals. However, disparities in organ access have been a serious issue for more than two decades. Geographic inequity in accessing liver transplantation across DSAs is well documented in the literature (see Yeh et al. 2011). In 2012, the OPTN board adopted a strategic plan that included reducing geographic disparities in accessing transplantation. Hughes (2015) provides an excellent summary of the laws enacted to improve liver allocation policies in the U.S.

1.1. Motivation

In June 2013, the Share 35 policy was introduced, with the intent of reducing waiting list mortality and addressing geographic disparities across DSAs. It allowed broader organ sharing for high-MELD patients beyond the local DSA (where the organ was recovered). The summary statistics show that while the waiting list mortality rate (number of patients who died on the waiting list divided by the number of new patients joining the waiting list) decreased from 12.0% in the Pre-Share 35 era to 9.4% in the Share 35 era, the median waiting time for a transplant increased by 5% (and its standard deviation across regions increased by 28%), and a greater fraction of transplants were offered to higher-MELD (transplants for MELD ≥29 patients increased from 44% to 52%) patients. However, the survival rates of patients with transplants in Table 1 from 2012 to 2015 indicate that higher MELD candidates have poorer survival outcomes. To sum up, determining the impact of the Share 35 policy is not straightforward. Our first *research objective* is to study the impact of the Share 35 policy on patient organ acceptance behavior (which is in response to the expected future value in the new policy). No previous work (to the best of our knowledge) has used an endogenous patient choice model to study this policy change. Moreover, building an

endogenous patient choice model is useful in its own right in evaluating other (counterfactual) allocation policies, which is a key objective of this paper.

Despite implementing broader organ sharing in a region for candidates with MELD scores ≥ 35 in 2013, geographic inequities have remained in the system. The highest reported median MELD score was 39 in Los Angeles, California (DSA: CAOP), and the lowest was 20 in Indianapolis, Indiana (DSA: INOP) (Kim et al. 2018). In July 2018, six waiting list patients in New York, California, and Massachusetts filed a lawsuit (Cruz et al. v. U.S. Dept. of Health and Human Services, S.D.N.Y 18-CV-06371) against the Health Resources and Services Administration (HRSA), an agency of the HHS. The lawsuit pointed out two main issues: 1. Significant geographic variability existed in the median MELD scores of candidates for deceased-donor transplants such that one's place of residence largely determined her chances of survival in the Share 35 policy; and 2. In the previous DSA-based Share 35 allocation policy (due to rigid boundaries), it was possible for an organ to be offered to a less sick candidate in a more distant transplant center over a sicker candidate in a closer transplant center. HRSA has already been under pressure over the last two decades to address geographic disparities (Hughes 2015). The lawsuit precipitated a change from the Share 35 allocation policy to the Acuity Circles policy in February 2020. The new policy addressed the second issue of the lawsuit. Nevertheless, it is unclear whether the first issue (i.e., geographic inequity) will be addressed by the new policy.[1] Our second *research objective* is to study whether the current Acuity Circles policy is better than the Share 35 policy in terms of geographic equity and efficiency metrics.

Managing the trade-off between equity and efficiency has been a very active area for researchers (see Section 3) and policymakers. Recent policies are moving toward broader sharing in principle. To provide some perspective, the Pre-Share 35 policy historically allowed organ sharing mainly within the DSA (the average distance between the donor hospital and the transplant center (TC) pairs within the same DSA is 66 nautical miles (NM)). After that, the Share 35 policy allowed organ sharing at the regional level for sicker patients (the average distance between the donor hospital and the TC pairs within the same region is 262 NM). The current Acuity Circles policy allows organ sharing up to 500 NM for sicker patients. The future policy framework aims to further increase this distance. Our third and final *research objective* is to investigate whether there is a better alternative (in making an equity-efficiency trade-off) than broader organ sharing as currently implemented. Overall, our unique study fills a knowledge gap by evaluating an earlier policy's impact and using the insights gleaned to propose a new policy.

[1] Due to the pandemic, data on the current Acuity Circles policy would not be useful because hospital resources were shifted to COVID treatment. Moreover, the priorities of the waiting list transplant patients also changed in light of the new situation.

To assess a new proposal and predict its impact, the transplant community uses the Liver Simulated Allocation Model (LSAM).[2] One of its main shortcomings is that it cannot model forward-looking behavior in a patient due to a new policy (more in Section 6.5). This model assumes the same organ acceptance probability function, irrespective of policy, geography, or organ access. Goel et al. (2018) compared the LSAM predictions due to the Share 35 policy with the actual results observed. They found that LSAM overestimated the increase in the transplant rates for MELD/PELD ≥ 35 candidates (46% predicted versus 36% observed), and underestimated the decrease in the transplant rates for MELD/PELD 30-34 candidates (1% predicted versus 33% observed). Prior research (Su and Zenios 2005) has also shown that ignoring a patient's choice leads to overestimating the efficiencies.

1.2. Contributions

Our paper makes the following key contributions to the literature. First, we build a structural model and provide a framework to analyze a patient's strategic response to a policy change in the context of liver transplantation. Our model is based on approximately 40 medical characteristics of patients and donors. We use the *logit inclusive value* technique to make the analysis computationally tractable (see Section 5.3). Our model's predictions are much better than the existing model (LSAM) and other reduced-form models (see Section 6.5). Secondly, we use our model to give accurate policy evaluations to inform decision makers.

The findings are as follows: 1. We perform a comparative study of the Pre-Share 35 and Share 35 policies and demonstrate the heterogeneity in the behavioral (i.e., organ acceptance probability) change of patients as a function of their region and MELD scores. We find that sicker patients benefited and became more selective in their behavior (i.e., their organ acceptance probability decreased for the same organ in consideration). However, there was heterogeneity in the behavioral change across geographies in less sick patients. Overall, the Share 35 policy reduced geographic disparity compared to its predecessor policy; 2. The Acuity Circles policy was implemented in February 2020 to 'improve' upon the 'Share 35' policy. We observe that, compared to the Share 35 policy, the Acuity Circles policy performs very similarly in geographic equity metrics but results in more offer refusals and a lower transplant benefit; and 3. We illustrate that broader sharing in its current form may not be the best strategy for balancing geographic equity and efficiency. The intuition is that by indiscriminately enlarging the pool of supply locations from where patients can receive offers, these patients tend to become more selective, resulting in more offer rejections and less efficiency. We suggest an alternative approach, one that equalizes the supply (deceased donors)-to-demand (waiting list patients) ratios across geographies by selectively increasing the

[2] `https://www.srtr.org/requesting-srtr-data/simulated-allocation-models/` accessed on July 12, 2020.

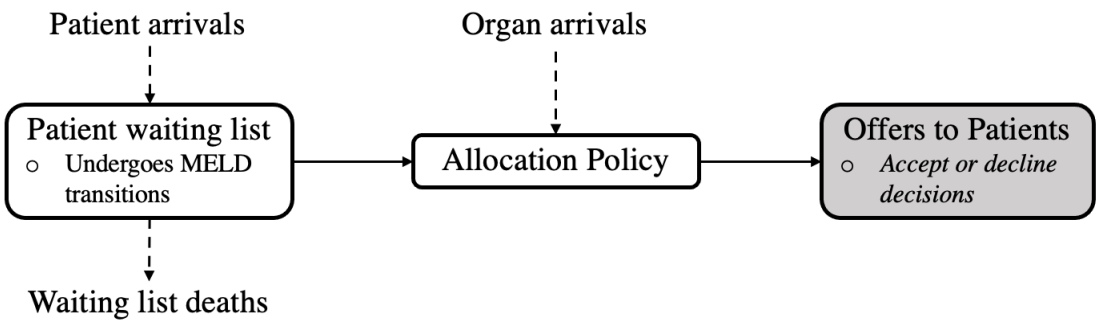

Figure 2 **Flowchart of deceased-donor organ allocation process in the U.S.**

sharing radius around donor hospitals. We show that this approach has the highest efficiency among the policies studied while improving upon geographic equity measures.

The structure of the rest of this paper is as follows. In the next section, we provide a brief overview of the liver allocation system in the U.S. Section 3 reviews the relevant literature. Section 4 describes the data and a few model-free pieces of evidence regarding behavioral change. Section 5 presents our optimization model. Section 6 describes our estimation procedure and results. Section 7 performs a counterfactual study comparing various allocation policies, including our proposed alternative 's/d Match'. Finally, we summarize and conclude in Section 8.

2. Liver Allocation Policy

UNOS supervises the transplantation network in the U.S. Its primary responsibilities include managing the national transplant waiting list, matching organs from deceased donors to candidates, establishing the medical criteria for allocating organs, facilitating organ distribution, framing equitable policies, and so forth. Some of the main UNOS members are the 142 liver transplant centers (TCs) and Organ Procurement Organizations (OPOs) in the 58 DSAs. The OPO coordinates the local procurement of deceased-donor organs and allocation within a DSA.

Figure 2 shows the flowchart of deceased-donor liver allocation for transplantation. A TC evaluates a candidate and decides whether or not to add her to the waiting list. The medical data of the candidates are shared with UNOS. These pooled data of candidates across all transplant hospitals are constantly updated when new candidates are added, and existing candidates are either removed or their medical conditions (e.g., MELD scores) are updated. When a deceased-donor organ becomes available, the OPO sends the organ donor's medical data to UNOS. Subsequently, the UNOS matching system compares the donor information with the candidate pool to rank candidates for organ offers according to the allocation policy. Upon receiving an offer, the transplant surgeon or physician, in consultation with the candidate, decides whether to accept the offer. The only clinically approved preservation method in the case of a liver is simple cold storage (see

Lee and Mangino 2009). Because organs lose viability due to a lack of oxygen, a liver often gets discarded after around 10-12 hours after its recovery.

Now, we describe the allocation policies that we consider in this study.

2.1. Previous Policies

The first objective scoring system adopted by OPTN/UNOS was the Child-Turcotte-Pugh (CTP) score in 1998. However, this score was not effective in discriminating the illness severity (Smith et al. 2012). Since February 2002, MELD has been used in allocation policies to quantify the urgency level. Table 2 compares the policy in place before and after June 2013 (until February 4, 2020) for adult donors. We refer to the policy before June 2013 as the Pre-Share 35 policy. The Share 35 policy brought about the following two changes: it increased the priority of regional patients with a MELD $\geq$35 and prioritized high-MELD national patients over low-MELD ($<$15) local/regional patients. Because the Share 35 policy led to prioritizing sick patients registered outside the DSA and region, it can be seen as a broader sharing policy. In the above policies, the offer-priority hierarchy is based on the MELD and sharing type (local/regional/national).

2.2. Current Policy: Acuity Circles

This policy progressively shares organs in circle radii of 150 NM, 250 NM, and 500 NM around the donor hospital, with the following hierarchy: (1) Status 1 candidates at TCs within 500 NM; (2) candidates with a MELD $\geq$37 within 150 NM, then 250 NM, and then 500 NM; (3) candidates with a MELD $\geq$33 within 150 NM, then 250 NM, and then 500 NM; (4) candidates with a MELD $\geq$29 within 150 NM, then 250 NM, and then 500 NM; (5) candidates with a MELD $\geq$15 within 150 NM, then 250 NM, and then 500 NM, then nationally; (6) candidates with a MELD $<$15 within 150 NM, then 250 NM, then 500 NM, and then nationally. This is a 'one-size-fits-all' policy, as it does not account for the organ arrival rate, candidate waiting list, or distances of the TCs from a donor hospital.

Sequence #	Pre-Share 35	Share 35
1	Status 1 (local)	Status 1 (local)
2	Status 1 (regional)	Status 1 (regional)
3	MELD $\geq$15 (local)	MELD $\geq$35 (local and regional, with preference to local candidates at each MELD)
4	MELD $\geq$15 (regional)	MELD $\geq$15 (local)
5	MELD $<$15 (local)	MELD $\geq$15 (regional)
6	MELD $<$15 (regional)	Status 1 (national)
7	Status 1 (national)	MELD $\geq$ 15 (national)
8	MELD $\leq$40 (national)	MELD $<$15 (local)
9	-	MELD $<$15 (regional)
10	-	MELD $<$15 (national)

Table 2 Comparison of deceased-adult donor allocation policies. Local (regional) refers to the donor and candidate belonging to the same DSA (region), and national in the case of different regions.

2.3. Supply-to-demand (s/d) Match Policy

We use the optimization framework proposed in Akshat et al. (2022) and apply the *maximin* principle to design heterogeneous radii circles that maximize the minimum value of the supply-to-demand (s/d) ratio across all TCs. The s/d Match policy adheres to the Final Rule and the principles adopted by the UNOS board in 2018 for all future organ policies.[3] We set the minimum and maximum circle radii around the donor hospitals to be 150 NM and 500 NM (in line with the innermost and outermost radii used in the Acuity Circles policy) as an illustration. Based on the setup considered in Section 7, the optimized set of circles results in a minimum (maximum) s/d ratio (at the TC level) of 0.58 (0.83). In contrast, if we consider 500 NM circles around every donor hospital, the s/d ratio range is 0.45-1.14. (We note that a tighter s/d range can be obtained by changing the maximum radius value. See EC.13 for details on the s/d range and performance measures when we allow the maximum radius around the donor hospital to be 600 NM.)

2.4. National Sharing Policy

As the name suggests, candidates are first ranked based on their MELD scores, irrespective of their location in the U.S. In the case of a tie (i.e., conditional on the MELD), local candidates are preferred over regional candidates, and regional candidates are preferred over candidates outside the region (we set this preference order because Feng et al. (2006) document the increased risk of graft failure from local to regional, and from regional to national sharing). Therefore, we try to mitigate (although not eliminate entirely) the role of one's location through this policy. We note that this policy might involve long-distance travel and may not be an appealing or practical idea, given that it may increase the chance of the organ being discarded.[4]

3. Related Research

There are three main streams of literature relevant to our study: 1. Proposals to address geographic disparities, 2. Efficiency-equity trade-offs, and 3. Dynamic optimization modeling in organ transplantation.

Redistricting has been proposed by many researchers in the operations community to address the issue of geographic inequity. Redistricting is a problem that occurs frequently in multiple domains (e.g., political redistricting, school redistricting, and sales territory assignment) where a finite, denumerable set of non-overlapping geographic units are aggregated into regions/districts subject to some criteria. Hess et al. (1965) and Garfinkel and Nemhauser (1970) introduced the use of

[3] `https://optn.transplant.hrsa.gov/media/2506/geography_recommendations_report_201806.pdf`, accessed April 30, 2022.

[4] Implementing a National Sharing policy is likely to increase CIT substantially. Although Gentry et al. (2014) concluded that the estimated transport time for livers comprised only 21% of the CIT, we note that their model was based on historical data.

optimization techniques for political redistricting. Stahl et al. (2005) considered geographic equity as measured using intraregional transplant rates in their objective function, along with efficiency (measured by total intraregional transplants), but they restrict their regions to contain up to eight DSAs due to computational challenges. Extending their work, Demirci et al. (2012) developed a branch-and-price algorithm to incorporate a larger set of potential regions and explored the efficient frontier in a trade-off between efficiency and geographic equity. Gentry et al. (2015) used optimization to reorganize DSAs into regions/districts to reduce geographic disparities. Working closely with the liver committee of UNOS, they proposed eight-district and four-district (reorganized DSA) maps. The proposed maps were under active consideration by UNOS from 2015 to 2017, but ultimately after significant debate and public comment, they were not adopted. Kilambi and Mehrotra (2017) introduced the neighborhood framework in organ allocation as a way to provide for broader sharing and improve geographic equity. Each DSA has its own neighborhood consisting of a unique set of other DSAs (or neighbors) with which it shares its organs. Rectifying the shortcomings in the supply-to-demand ratio measure used by Kilambi and Mehrotra (2017), Akshat et al. (2022) proposed heterogeneous circles around donor hospitals to create an equitable geographic distribution by developing a scalable set-partitioning optimization model. Ata et al. (2017) used fluid approximation and game theory to show that multi-listing (a patient is listed at more than one TC, potentially in other DSAs or regions, so that she can get organ offers from multiple places) can reduce geographic disparity in kidney allocation. However, fewer than 2% of patients (on April 14, 2021, the OPTN website showed that fewer than 181 out of 11,868 candidates were multiple listed) waiting for a liver transplant were multi-listed. Moreover, multi-listing would not make the system fair; indeed, it would instead create disparity based on a candidate's economic means. Bertsimas et al. (2020) suggest using trade-off curves to assess three organ distribution frameworks identified by UNOS. Running a massive number of simulations for the three distribution frameworks,[5] they plotted trade-off curves of efficiency (measured as the average travel distance) versus fairness (measured as deaths or variance in the median MELD at the time of the transplant). For a given value of the efficiency metric, the trade-off curve then identifies the policy with the greatest fairness. Most of the above studies rely on LSAM to assess the performance of their proposals, owing to policymakers' reliance on it. LSAM is a sophisticated patient-level simulation that handles MELD scores and models whether a candidate accepts or declines an offer (Thompson et al. 2004). However, it ignores the heterogeneity in patients' organ acceptance behavior and its dependence on the policy.

[5] `https://optn.transplant.hrsa.gov/media/2565/geography_publiccomment_201808.pdf` accessed on July 1, 2022.

Zenios et al. (2000) study the trade-off between clinical efficiency (measured as Quality Adjusted Life Years (QALY)) and equity (types of patients defined based on their demographics) in the kidney allocation problem using a fluid model and ignoring patients' choices. They propose a heuristic dynamic index policy to maximize the multi-criteria objective function. Su and Zenios (2005) use a sequential assignment model (of n transplant patients and n kidneys) to investigate the impact of a patient's choice in the kidney allocation system. They focus on a social planner's objective of maximizing the overall social welfare and conclude that ignoring the patient's choice leads to overestimating the efficiencies in the policies they studied. Bertsimas et al. (2012) study the α-fairness scheme (see Atkinson 1970) to trade off efficiency and fairness. Their measure of efficiency is the sum total of utilities, and they do not focus on geographic disparity. Su and Zenios (2006) find that introducing information asymmetry (the transplantation system does not know the post-transplant outcome, which is known to the patient) in the allocation policy achieves an overall outcome in the middle of the efficiency-equity spectrum. Bertsimas et al. (2013) proposed a method to design a point-based kidney allocation system, where policymakers can select the fairness constraints. This method maximizes the medical efficiency (captured using life-years gained from the transplant); however, Bertsimas et al. test policies assuming an exogenous organ acceptance model for patients. Arikan et al. (2018) use a probit model to elicit differences in the intent for organ (kidney) procurement at the level of DSAs between marginal-quality organs and the rest. They conclude that geographically broader sharing of the bottom 15% quality kidneys can help enhance the kidney supply.

Other papers (Washburn et al. 2016, Goldberg et al. 2017) have studied the effect of the Share 35 policy using logistic regression model, which is not appropriate for studying the dynamic optimization problem setting. Zhang (2010) is the closest paper to ours in terms of the methodology. Their focus is on studying the presence of observational learning in patient behavior regarding the deceased-donor kidney allocation process. Agarwal et al. (2021) and Ata et al. (2022) study deceased-donor kidney allocation policies using structural models. Besides the difference in the context (liver versus kidney), there are three key differences between these two papers and ours. First, in addition to transplantation, dialysis is also a treatment option for kidney failure. Second, these two papers assume patient health transitions to be deterministic, whereas we model the stochastic transition of MELD scores. Third, the liver allocation policy evolution presents a unique opportunity to study the impact of broader sharing on patient outcomes. Furthermore, Agarwal et al. (2021) do not study geographic disparity. Alagoz et al. (2007b) use a discrete-time, infinite-horizon discounted Markov decision process model to study the patient's decision to accept an offer or wait. They find that the optimal policy is typically of the control-limit type. However, they also assume a fixed cost of waiting, whereas our model uses a richer set of variables to model

the utility and waiting cost. In addition, their model assumes the same reward (or utility) from local, regional or national offers whereas our model allows for different utilities from these offers.

4. Data and Evidence

4.1. Data

This study used data from the Scientific Registry of Transplant Recipients (SRTR). The SRTR data system includes data on all donors, wait-listed candidates, and transplant recipients in the U.S., submitted by the members of the Organ Procurement and Transplantation Network (OPTN). The Health Resources and Services Administration (HRSA), U.S. Department of Health and Human Services provides oversight to the activities of the OPTN and SRTR contractors.

The four main datasets used in the study are candidates' information at the time of registration, the transition of their MELD scores while waiting, donor information, and the candidates' decisions regarding organ offers. We use nine years (2010 to 2018) of candidate and donor information in our structural model analysis. This covers both the Pre-Share 35 and Share 35 policy eras. We restrict our analysis to deceased-donor organs from adult donors and to adult candidates (allocation policies are different for donors <18 years). Because we are interested in analyzing geographic disparity across policies, we use data from all 11 regions. For the purpose of estimating MELD transitions, we use a larger dataset of 16 years (January 2003 to February 2019). EC.1 provides the summary statistics of a few key variables in the data.

4.2. Model-Free Evidence of Behavioral Change

Figure 3 compares the MELD at the time of an offer and at the time of a transplant (of candidates who accepted the offer) between the Pre-Share 35 and Share 35 policies using box plots. Consistent with the Share 35 policy that prioritizes sicker patients, the MELD at the time of an offer increased. The MELD at the time of a transplant also increased slightly, suggesting that a greater number of sicker patients received transplants, and therefore, avoided death. However, the relative increase in the MELD at the time of a transplant is smaller than the MELD at the time of an offer, suggesting more offer refusals. One may wonder whether these refusals are due to lower-quality organs being offered, or whether the candidates became more selective in their behavior. We find no significant differences in the organ quality of the declined offers between the two policy eras (see EC.2). Thus, it is likely that the refusals are due to behavioral change. Offer refusals tend to increase the waiting time for an organ transplant, thereby deteriorating the organ quality (and its utility from transplantation). On the one hand, the Share 35 policy seems to save more lives, while it may lead to a decrease in transplant quality (in terms of the graft survival probability) due to more offer rejections on the other hand. Further, we also see interaction effects. Conditional on offers to candidates with a MELD <35 (MELD ≥35), the average MELD at an offer acceptance increased

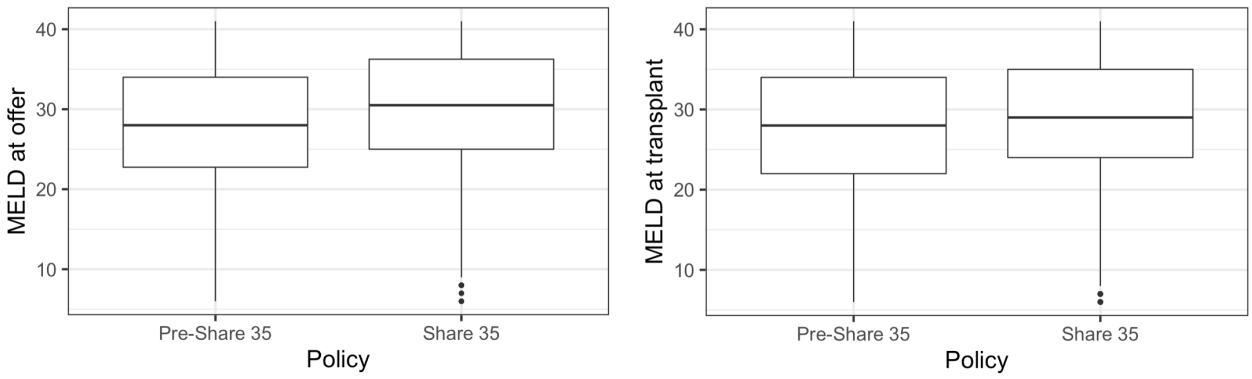

Figure 3 **Comparison of MELD at the time of an offer and a transplant between policies using box plots (Status 1A is assigned a MELD score of 41).**

(decreased) by 0.68 (0.43). Next, we use a straightforward metric to calculate the acceptance probability (ratio of the number of offers accepted and the number of offers received). Table EC.2 reports the change in acceptance probabilities as a function of MELD in different regions. We see cases of both an increase and decrease in their acceptance probabilities.

5. Patient's Dynamic Choice Model

We now describe the choice model of a patient. When the patient is offered an organ, she evaluates the utility (in terms of her survival chances) derived from that organ and decides to either accept it and undergo transplantation or decline it and wait for the next offer (anticipating a better one). A patient, in consultation with a transplant surgeon, evaluates an offer (for confidentiality reasons, the SRTR data does not contain surgeon-level information). While waiting, her health state will evolve stochastically, affecting her priority for future offers. In accordance with the allocation policy in the U.S., there is no implication of a patient's offer refusal on her future offers. Now, we formally introduce our model. Table 3 describes the notation used in the formulation.

We model the patient's problem as a discrete-time infinite-horizon dynamic optimization problem, where she faces the trade-off between accepting the current offer and waiting for future offers. We consider the Markov perfect equilibrium, and patients account for only payoff-relevant variables, compositely represented by S_{it}, in their decision-making.

Upon accepting an offer, a patient receives an expected utility of $EU(S_{it})$ and is removed from the waiting list (and we assume that she never joins again). $EU(S_{it})$ captures the expected present discounted payoff from accepting an offer (in state S_{it}). If a patient declines the offer, then she incurs an immediate waiting cost (as modeled in Section 5.2) and expects to receive some utility in the future (as modeled in Section 6.1.1). Formally, the Bellman equation for patient i's dynamic optimization problem at time t is

Notation	Description
i	Patient
$t = 1, ..., \infty$	Organ arrival time (in days)
δ	Daily discount factor
Payoff-relevant variables	
Candidate specific variables:	
$MELD_{it}$	MELD score of patient i at time t
Rec_age_{it}	Candidate i's age group at time t
$Rec\_life\_support_{it}$	Candidate i's life support status ('Yes' or 'No') at time t
$Rec\_med\_cond_{it}$	Candidate i's medical condition ('ICU': Intensive Care Unit, 'H': Hospitalized, or 'NH': Not Hospitalized) at time t
Organ specific variables:	
Don_age_{it}	Age of the donor whose organ is offered to candidate i at time t
Don_race_{it}	Race of the donor whose organ is offered to candidate i at time t
Don_cod_{it}	Cause of death of the donor whose organ is offered to candidate i at time t
Don_dcd_{it}	Indicates donation after circulatory death ('Yes' or 'No') of the donor whose organ is offered to candidate i at time t
Joint candidate-donor variables:	
Z_{it}	Candidate's and donor's medical attributes used in the SRTR Risk Adjustment Model (uses 41 attributes)
GS_{it}	One-year graft survival probability modeled as a function of $(MELD_{it}, Rec\_age_{it}, Rec\_life\_support_{it}, Rec\_med\_cond_{it}, Q_{it})$
$Sharing\_type_{it}$	Denotes whether the organ offer (with respect to patient i's DSA) at time t is classified as *local*, *regional*, or *national* sharing
Q_{it}	$(Don\_age_{it}, Don\_race_{it}, Don\_cod_{it}, Don\_dcd_{it})$
S_{it}	$(MELD_{it}, Rec\_age_{it}, Rec\_life\_support_{it}, Rec\_med\_cond_{it}, Q_{it}, Z_{it}, Sharing\_type_{it})$
$\mathcal{P}(S_{i,t+1}\|S_{it})$	Transition probability of candidate i's state from t to $t+1$
Payoff functions	
$U_{it}(S_{it})$	Utility to candidate i upon accepting an offer at time t
$W_{it}(S_{it})$	One period of candidate i's waiting cost at time t
$V(S_{it})$	Patient's maximum expected present discounted value associated with state S_{it}
Decision variable	
d_{it}	1 if candidate i accepts the offer at time t, and 0 otherwise

Table 3 Model Notation

$$V(S_{it}) = \max \left\{ EU(S_{it}), -EW(S_{it}) + \delta \sum_{S_{i,t+1}} \mathcal{P}(S_{i,t+1}|S_{it}, d_{it} = 0) \times V(S_{i,t+1}) \right\} \tag{1}$$

5.1. Utility Function

We consider a linear functional form for modeling the utility associated with a candidate-donor pair. For a pair, we estimate the graft survival probability using the SRTR Risk Adjustment Model,[6] which is based on a total of 41 predictors (Z_{it}) that include the candidate's and donor's

[6] `https://www.srtr.org/reports-tools/posttransplant-outcomes/` accessed on July 12, 2020.

medical attributes, and CIT. Using the post-transplant outcome in the utility is in line with the extant literature (Su and Zenios 2006). Moreover, we believe that a patient would be interested in maximizing her eventual survival outcome (post-transplantation) without incorporating her survival chance without a transplant. The CIT is realized and observed only for transplants that took place. Predicting CIT for an offer is very difficult primarily due to the nonavailability of data on the mode of organ transport (driving, helicopter, or fixed-wing), and non-transport factors (such as back-table preparation) at the SRTR (Gentry et al. 2014). We set CIT equal to its median value (=6.9 hours) both in Z_{it} and the graft survival probability function (SRTR Risk Adjustment Model), and include the *Sharing_type* variable to capture the effect of the elapsed time between organ recovery and transplantation on the (prospective) transplant quality. We model the utility of the transplantation to be derived from the one-year graft survival probability (GS_{it} to be precise; see Section 5.3 for details) and the $Sharing\_type_{it}$, which captures the effect of CIT. The utility to patient i at time t is given by:

$$U_{it}(S_{it}) = \begin{cases} \beta_0 + \beta_{GS} GS_{it} + \beta_{Sharing}\, Sharing\_type_{it} + \epsilon_{it}, & \text{if candidate } i \text{ accepts the organ at time } t, \\ \epsilon_{it}. & \text{otherwise.} \end{cases} \tag{2}$$

GS_{it} and $Sharing\_type_{it}$ are observable to both patient i. β_{GS} and $\beta_{Sharing}$ are the associated utility parameters; β_0 is the intercept. ϵ_{it} denotes the idiosyncratic utility shock experienced by patient i while evaluating the offer at time t. It represents the random factors (playing a role in the decision-making) that are unobserved to the econometrician such as weather conditions, momentary inconvenience to the patient, surgery-related factors, randomness involved in the survival probability assessment, etc. ϵ_{it} is assumed to follow an independent and identically distributed (i.i.d.) Gumbel distribution across patients and offers. We subtract $E(\epsilon_{it})$, a constant, from the utility so that the expected utility upon accepting an offer is given by:

$$EU(S_{it}) = \beta_0 + \beta_{GS} GS_{it} + \beta_{Sharing}\, Sharing\_type_{it} \tag{3}$$

5.2. Waiting Cost Function

A candidate incurs a waiting cost if she declines the offer or does not receive one at time t. To model her waiting cost, we use variables such as age, life support status, and medical condition. ω_{Age}, ω_{LS}, and ω_{MC} are the associated waiting cost parameters. Given that *Death* is an undesirable and terminal state, we add the term $\mathbb{1}_{\{MELD_{it}=Death\}}$ to the waiting cost function such that a patient incurs a one-time expected cost of $\frac{1}{1-\delta} \times \omega_d$ upon *Death*. Formally,

$$W_{it}(S_{it}) = \begin{cases} \omega_d + \epsilon_{i0t}, & \text{if candidate dies at time } t, \\ \omega_{Age}\, Rec\_age_{it} + \omega_{LS}\, Rec\_life\_support_{it} + \omega_{MC}\, Rec\_med\_cond_{it} + \epsilon_{i0t}. & \text{otherwise.} \end{cases} \tag{4}$$

where ϵ_{i0t} is an independent and identically distributed (i.i.d.) Gumbel distribution across patients and times. We subtract $E(\epsilon_{i0t})$, a constant, from the function so that the expected waiting cost is given by:

$$EW(S_{it}) = \mathbb{1}_{\{MELD_{it}=Death\}}\omega_d + \mathbb{1}_{\{MELD_{it}\neq Death\}}[\omega_{Age}\, Rec\_age_{it} + \omega_{LS}\, Rec\_life\_support_{it} + \omega_{MC}\, Rec\_med\_cond_{it}] \quad (5)$$

5.3. (Simplifying) State Transition Probability

In our dynamic model, patients have perceptions over future states. They need to know the evolution of every element in the state space, including Z_{it}. Following the extant literature on the *logit inclusive value* (Gowrisankaran and Rysman 2012), we make a simplifying assumption: the evolution of Z_{it} is approximated using a one-dimensional GS_{it}. In doing so, we consider a patient to be boundedly rational, and they use fewer elements to form predictions about the future.

We model GS_{it} as a function of $(MELD_{it}, Rec\_age_{it}, Rec\_life\_support_{it}, Rec\_med\_cond_{it}, Q_{it})$. We group the offers by $(MELD_{it}, Rec\_age_{it}, Rec\_life\_support_{it}, Rec\_med\_cond_{it}, Q_{it})$, and GS_{it} is the average of the graft survival probabilities (calculated using the respective Z_{it}'s) for these offers. Thus, we only need the evolution of GS_{it}, which is relatively easier to estimate than the evolution of Z_{it}. EC.3 provides details.

If a patient declines an offer or does not receive one, she transitions to a new state on the next day. EC.4 gives the detailed expression for $\mathcal{P}(S_{i,t+1}|S_{it}, d_{it}=0)$.

5.4. Offer Acceptance Probability

It follows from the i.i.d. Gumbel assumption of the idiosyncratic shocks in the payoff functions, and the fact that the difference of two Gumbel-distributed random variables follows a logistic distribution, that the logit choice probability of accepting an offer is:

$$P(\text{accepting an offer}|S_{it}) = \frac{e^{EU(S_{it})}}{e^{EU(S_{it})} + e^{-EW(S_{it})+\delta\sum_{S_{i,t+1}}\mathcal{P}(S_{i,t+1}|S_{it},d_{it}=0)\times V(S_{i,t+1})}}, \quad (6)$$

where $EU(.)$ and $EW(.)$ represent the expected utility and waiting cost, respectively.

6. Model Estimation

In this section, we describe the estimation procedure, parameter identification, and results. Our estimation framework closely follows Zhang (2010), in combination with the *logit inclusive value* technique of Gowrisankaran and Rysman (2012) to make our model tractable.

6.1. Estimation Procedure

We estimate the model using the nested fixed point algorithm (Rust 1987). First, given a set of parameter values, an 'inner' algorithm computes the value function, $EV(S_{it})$. Then, the log-likelihood function is calculated using the parameter values and the value function vector. An 'outer' algorithm chooses the next set of parameters to maximize the log-likelihood function.

6.1.1. Value Function. The value function, denoted by $EV(S_{it})$, is defined as the total future value that candidate i expects to receive when she waits (declines or does not receive an offer) at time t. The future value depends on her state transition, and the expected payoff in the new state.

$$EV(S_{it}) = \sum_{S_{i,t+1}} \mathcal{P}(S_{i,t+1}|S_{it}, d_{it}=0) \times V(S_{i,t+1}) \tag{7}$$

Substituting equation (7) into equation (1), we get:

$$V(S_{it}) = \max\{EU(S_{it}), -EW(S_{it}) + \delta EV(S_{it})\} \tag{8}$$

Using the aggregation properties of the Gumbel distribution,

$$V(S_{it}) = \ln\left[e^{EU(S_{it})} + e^{-EW(S_{it})+\delta EV(S_{it})}\right] \tag{9}$$

We can rewrite the value function as follows:

$$EV(S_{it}) = \sum_{S_{i,t+1}} \mathcal{P}(S_{i,t+1}|S_{it}, d_{it}=0) \times \ln\left[e^{EU(S_{i,t+1})} + e^{-EW(S_{i,t+1})+\delta EV(S_{i,t+1})}\right], \tag{10}$$

where the second term under summation corresponds to the expected payoff when in state $S_{i,t+1}$.

The state space (described in Section 6.2) in our setting is discrete. Let K be the dimension of the state space, and let Π be a $K \times K$ Markov transition matrix of the state elements (calculated using equation EC.5). The value function can be concisely represented as:

$$EV(.) = \Pi \times \ln\left[e^{EU(.)} + e^{-EW(.)+\delta EV(.)}\right], \tag{11}$$

where $EV(.), EU(.)$, and $EW(.)$ are all $K \times 1$ vectors. This nonlinear system of equations can be solved iteratively using a fixed-point algorithm.

6.1.2. Log-Likelihood Function. We use the maximum likelihood estimation approach to estimate the structural model parameters. EC.5 describes the derivation and final expression of the log-likelihood function. We maximize the overall log-likelihood function, equation EC.11, to estimate the parameters (β_0, β_{GS}, $\beta_{Sharing}$, ω_d, ω_{Age}, ω_{LS}, and ω_{MC}).

6.2. Parameter Identification

Before we present the parameter estimates, we expand on some of the state variables. We discretize *Rec_age* into three groups: R1: < 45 years, R2: $(45-65)$ years, and R3: ≥ 65 years; *Don_age* into four groups: $(18-39)$ years, $(40-49)$ years, $(50-59)$ years, and ≥ 60 years; *Don_race* into 'White' and 'Others' categories; *Don_cod* into 'Anoxia', 'Cerebrovascular accident (CVA)', and 'Others' categories; *Rec_life_support* into 'Yes' and 'No'; *Rec_med_cond* into 'ICU' (Intensive Care Unit), 'H' (Hospitalized), and 'NH' (Not Hospitalized) categories; and *Don_dcd* into 'Yes' and 'No'.

The variable selection and discretization are primarily motivated by the medical literature (Schaubel et al. 2009, Feng et al. 2006). We categorize the MELD scores into six classes: MELD 6-14, MELD 15-28, MELD 29-32, MELD 33-34, MELD 35-36, and MELD >36, and add the terminal *Death* state. This creates a 7×7 MELD transition matrix (Table EC.3). The above classification of MELD scores provides sufficient granularity to evaluate the Pre-Share 35, Share 35, and Acuity Circles policies. Overall, there are 18 patient types, 49 organ types, and 15,678 elements in the state space; consequently, every geographic unit (DSA or TC, depending on the allocation policy) has its own $K \times K$ Markov transition matrix, where $K = 15{,}678$.

Now we discuss the identification of the structural model parameters. GS_{it} is a function of the MELD category, age group, life support status, medical condition, and organ type (see EC.3 for details). A variation in the accept/decline decisions of patients with their MELD score, and organ type is sufficient to identify β_{GS}. For example, patients might have a different probability of offer acceptance at a lower MELD score, keeping everything else (age group, life support status, medical condition, sharing type, and organ type) the same. This difference in the probability of offer acceptance can be attributed to the difference in GS_{it}. EC.6 provides more details on the identification of the parameter associated with GS_{it}.

We summarize the probability of acceptance (calculated as the ratio of the number of offers accepted and the number of offers received) for some of the variables that are part of the state space in Table 4. The variation in the acceptance probability enables the identification of the parameters associated with these variables in the structural model. After controlling for the candidate and donor-specific state variables, there exists variation in the sharing type (local/regional/national) of the offers. The differences in the candidates' acceptance behavior help identify $\beta_{Sharing}$. A candidate might die if she keeps declining offers and continues to wait. The MELD transition matrix, $\mathcal{P}(MELD_{i,t+1}|MELD_{it}, d_{it} = 0)$, enables us to identify ω_d. In the data, we have candidates of various age groups, life support statuses, and medical conditions. The variations in their offer acceptance behaviors facilitate the identification of the parameters (ω_{Age}, ω_{LS}, and ω_{MC}). We assume the daily discount factor, $\delta = 0.99$, in our estimation. Our value of δ is in line with that of Zhang (2010), who uses a discount factor of 0.99 for every six days (equivalent to a daily discount factor of 0.991).

Sharing type	P(%)	Candidate age group	P(%)	Candidate life support	P(%)	Candidate medical condition	P(%)
Local	9.0	R1	6.7	No	5.8	NH	5.5
Regional	4.4	R2	6.1	Yes	20.9	H	13.3
National	1.2	R3	5.2			ICU	24.5

Table 4 Summary statistics of probability of acceptance ($P :=$ # of offers accepted/# of offers received) for some of the variables in the state space. The variation in P enables the identification of the parameters associated with these variables in the structural model.

Variable	Parameter	Estimate	Standard Error
Utility Function:			
Intercept	β_0	-21.7803	0.3145
Sharing type: Regional	$\beta_{Sharing}$	-1.0348	0.0113
Sharing type: National		-2.3328	0.0243
Graft survival probability (GS)	β_{GS}	19.5200	0.3353
Waiting Cost Function:			
Death	ω_d	0.1160	0.0007
Candidate age group: R2 (45-65 years)	ω_{Age}	0.0057	0.0002
Candidate age group: R3 ($\geq$65 years)		0.0061	0.0003
Candidate life support: Yes	ω_{LS}	0.0134	0.0008
Candidate medical condition: H	ω_{MC}	0.0114	0.0004
Candidate medical condition: ICU		0.0229	0.0008
No. of observations = 890,402			
Log-likelihood = -173,630.9			

Table 5 Estimation results of the structural model.

6.3. Estimates

Table 5 reports the estimates of the structural model.[7] The estimates of the parameters associated with *Sharing_type:* Regional and *Sharing_type:* National (with respect to *Sharing_type:* Local) are negative, and national sharing is associated with the least utility. This is reasonable, given that local organs are generally associated with fewer prior refusals, and the organs outside the region are associated with a higher number of prior refusals; thus, are usually of lower quality and less desirable. In fact, Feng et al. (2006) found similar estimates (0.105 for regional sharing and 0.244 for national sharing, with respect to local sharing) in their estimation of the donor risk index (DRI), a measure of the riskiness of graft failure associated with a donor organ. The estimate of β_{GS} is positive, which is consistent with the fact that organs that provide better survival are more desirable. *Death* is associated with a positive estimate and translates to a candidate incurring a one-time expected cost of $\frac{1}{1-\delta} \times \omega_d$ (=11.6) upon death. We observe that the waiting cost increases with age (most likely due to a decrease in well-being and the chances of comorbidities). Thus, older patients are more likely to accept an offer. Patients on life support incur a higher waiting cost than their counterparts. Compared to patients who are not hospitalized, hospitalized patients incur more costs, and ICU patients incur double the cost, compared to hospitalized patients. A higher waiting cost indicates greater urgency in accepting an offer. As a test for robustness, we relax the assumption of a fixed value of CIT in the utility function, and report the parameter estimates in EC.7.

[7] We used Julia 1.5.3 and the KNITRO solver to estimate our model on a 3.2 GHz 6-Core Intel Core i7 MAC with 32 GB RAM. Due to the size of the problem, it took approximately two weeks to solve the model.

6.4. Insights from the Structural Model

Now we study how patients would react to the possibility of a transplant, both based on their health status and future prospects of being offered an organ. We use a stylized setup of two regions and three DSAs (Region A: DSA 1 and DSA 2; Region B: DSA 3), each with a single TC, in our numerical study to draw key insights. We compare five settings of demand and supply across the DSAs (Set 1,..., Set 5; see Table 6). Note that the future prospect (captured by $EV(S_{it})$) depends on the organ offer probability, which depends on the supply and demand in various geographies (e.g., DSAs) and on the allocation policy in place (we consider both Share 35 and Acuity Circles). For this reason, we study the effect of a change in supply and demand on a patient's organ acceptance behavior (the steady state equilibrium organ acceptance probabilities are estimated using Algorithm 1 in EC.8). By comparing the patient's organ acceptance behavior between these sets, we draw inferences of the effect of the supply and demand volume, and the s/d ratio.

We consider a single patient type (*Rec_age*: $(45-65)$ years, *Rec_life_support*='No', *Rec_med_cond*='NH'), and a single organ type (*Don_age*: $(18-39)$ years, *Don_race* = 'White', *Don_cod* = 'Others', *Don_dcd* = 'No'). They represent the most frequent patient and organ types. We simulate the organ and candidate arrivals for a two-year time period ($t = 1, ..., 730$).

The main insights are as follows: (1) When the s/d ratio differs between two DSAs, the difference (in terms of probability of offer acceptance) is greater for lower-MELD patients. The difference is attenuated at higher MELD scores due to the prioritization of higher-MELD patients through broader sharing (Share 35 and the Acuity Circles policy). If the s/d ratio decreases at a DSA, a patient reacts by becoming aggressive in organ acceptance behavior (i.e., the organ acceptance probability increases for the same organ). (2) Increasing the supply and demand volume (keeping the s/d ratio the same) in a DSA leads to an enlarged supply from where patients can receive an offer, which induces more selective behavior. This behavioral change is not merely limited to the DSA at which a change is made; indeed, it also has a spillover effect on other DSAs. EC.9 provides a detailed comparison.

6.5. Benchmarking

Our data cover two policy regimes (Pre-Share and Share 35). The observations (accept/decline decisions) provide ground truth, which provides an opportunity to conduct an out-of-sample comparison, i.e., training a model using the Pre-Share 35 policy era observations, and testing it on the Share 35 policy era. This lays the foundations of a strongly validated structural model, which we use to study counterfactual policies in the next section.

We compare various models (different versions of the dynamic and reduced-form models) on several important goodness-of-fit metrics in Table 7. In the category of dynamic models, we consider

		Set 1*		Set 2		Set 3		Set 4		Set 5	
		d	s/d	d	s/d	d	s/d	d	s/d	d	s/d
	Region A:										
	DSA 1	250	0.7	250	0.7	250	0.7	250	0.7	250	0.7
	DSA 2	250	0.7	250	0.5	250	0.7	350	0.7	250	0.7
	Region B:										
	DSA 3	500	0.7	500	0.7	500	0.5	500	0.7	700	0.7
Share 35:											
	DSA 1	[0.073, 0.073]		[0.074, 0.074]		[0.074, 0.074]		[0.073, 0.073]		[0.073, 0.073]	
MELD 6-14	DSA 2	[0.073, 0.073]		[0.076, 0.076]		[0.074, 0.074]		[0.073, 0.073]		[0.073, 0.073]	
	DSA 3	[0.072, 0.073]		[0.073, 0.073]		[0.077, 0.077]		[0.072, 0.073]		[0.072, 0.073]	
	DSA 1	[0.076, 0.077]		[0.079, 0.079]		[0.077, 0.078]		[0.076, 0.077]		[0.077, 0.077]	
MELD 15-28	DSA 2	[0.076, 0.077]		[0.084, 0.085]		[0.078, 0.078]		[0.074, 0.075]		[0.076, 0.077]	
	DSA 3	[0.074, 0.075]		[0.074, 0.075]		[0.086, 0.087]		[0.074, 0.074]		[0.072, 0.073]	
	DSA 1	[0.141, 0.144]		[0.143, 0.146]		[0.143, 0.147]		[0.136, 0.141]		[0.137, 0.141]	
MELD 29-32	DSA 2	[0.139, 0.143]		[0.149, 0.153]		[0.145, 0.149]		[0.129, 0.134]		[0.135, 0.139]	
	DSA 3	[0.124, 0.128]		[0.126, 0.13]		[0.137, 0.14]		[0.12, 0.124]		[0.112, 0.117]	
	DSA 1	[0.271, 0.28]		[0.273, 0.282]		[0.275, 0.289]		[0.256, 0.27]		[0.254, 0.266]	
MELD 33-34	DSA 2	[0.266, 0.277]		[0.276, 0.287]		[0.278, 0.291]		[0.246, 0.263]		[0.252, 0.264]	
	DSA 3	[0.241, 0.256]		[0.247, 0.261]		[0.258, 0.269]		[0.231, 0.24]		[0.222, 0.234]	
	DSA 1	[0.467, 0.486]		[0.469, 0.486]		[0.473, 0.492]		[0.441, 0.467]		[0.438, 0.46]	
MELD 35-36	DSA 2	[0.464, 0.48]		[0.471, 0.487]		[0.483, 0.501]		[0.432, 0.462]		[0.431, 0.459]	
	DSA 3	[0.437, 0.46]		[0.447, 0.467]		[0.456, 0.472]		[0.426, 0.444]		[0.416, 0.435]	
	DSA 1	[0.694, 0.718]		[0.697, 0.717]		[0.702, 0.724]		[0.667, 0.697]		[0.663, 0.686]	
MELD >36	DSA 2	[0.687, 0.704]		[0.694, 0.71]		[0.705, 0.724]		[0.661, 0.691]		[0.657, 0.688]	
	DSA 3	[0.666, 0.687]		[0.681, 0.697]		[0.682, 0.701]		[0.661, 0.679]		[0.648, 0.669]	
Acuity Circles#:											
	DSA 1	[0.073, 0.073]		[0.074, 0.074]		[0.074, 0.074]		[0.073, 0.073]		[0.073, 0.073]	
MELD 6-14	DSA 2	[0.072, 0.073]		[0.076, 0.076]		[0.074, 0.074]		[0.072, 0.073]		[0.073, 0.073]	
	DSA 3	[0.073, 0.073]		[0.073, 0.074]		[0.077, 0.077]		[0.073, 0.073]		[0.073, 0.073]	
	DSA 1	[0.076, 0.077]		[0.079, 0.079]		[0.078, 0.079]		[0.076, 0.077]		[0.076, 0.077]	
MELD 15-28	DSA 2	[0.076, 0.077]		[0.083, 0.084]		[0.079, 0.079]		[0.074, 0.075]		[0.076, 0.077]	
	DSA 3	[0.074, 0.075]		[0.075, 0.076]		[0.085, 0.086]		[0.074, 0.074]		[0.072, 0.073]	
	DSA 1	[0.133, 0.136]		[0.135, 0.138]		[0.137, 0.141]		[0.126, 0.131]		[0.126, 0.132]	
MELD 29-32	DSA 2	[0.131, 0.136]		[0.137, 0.141]		[0.138, 0.143]		[0.123, 0.128]		[0.125, 0.129]	
	DSA 3	[0.122, 0.127]		[0.125, 0.129]		[0.134, 0.137]		[0.118, 0.122]		[0.111, 0.115]	
	DSA 1	[0.26, 0.27]		[0.261, 0.271]		[0.266, 0.281]		[0.24, 0.256]		[0.237, 0.252]	
MELD 33-34	DSA 2	[0.253, 0.266]		[0.259, 0.272]		[0.268, 0.282]		[0.237, 0.255]		[0.236, 0.249]	
	DSA 3	[0.239, 0.255]		[0.245, 0.259]		[0.254, 0.266]		[0.229, 0.238]		[0.22, 0.233]	
	DSA 1	[0.468, 0.488]		[0.466, 0.485]		[0.473, 0.493]		[0.441, 0.468]		[0.433, 0.457]	
MELD 35-36	DSA 2	[0.462, 0.48]		[0.471, 0.487]		[0.484, 0.502]		[0.43, 0.461]		[0.424, 0.455]	
	DSA 3	[0.436, 0.46]		[0.446, 0.466]		[0.453, 0.471]		[0.423, 0.443]		[0.414, 0.434]	
	DSA 1	[0.696, 0.721]		[0.697, 0.72]		[0.702, 0.726]		[0.667, 0.698]		[0.66, 0.685]	
MELD >36	DSA 2	[0.687, 0.706]		[0.696, 0.713]		[0.706, 0.727]		[0.66, 0.692]		[0.652, 0.688]	
	DSA 3	[0.667, 0.689]		[0.682, 0.698]		[0.684, 0.704]		[0.661, 0.681]		[0.649, 0.67]	

Table 6 Demand and Supply settings used in a numerical study to analyze their effect on a patient's behavior. *: Set 1 is the baseline setting. 95% confidence intervals of the average probability of organ acceptance are shown in square brackets. #: To model the Acuity Circles policy in this geographic setup of two regions and three DSAs, we assume local → Regional → National sharing (instead of different circular bands of radii 150, 250, and 500 NM) within each MELD category.

Measure	Dynamic Models			Reduced-form Models		
	Full Model	DM1	DM2	RM1	RM2	RM3
AUC (ROC)	0.772	0.694	0.772	0.756	0.728	0.762
AUC (PRC)	0.202	0.166	0.197	0.194	0.141	0.182
Log-likelihood	-118,076.2	-125,045.4	-118,792.5	-119,525.8	-124,941.3	-121,758
RMSE	0.224	0.227	0.225	0.225	0.229	0.227
MAE	0.103	0.110	0.106	0.101	0.102	0.116

Table 7 Comparing the goodness-of-fit (out-of-sample) of various models on threshold-independent measures. AUC (ROC) and AUC (PRC) are the area under the receiver operating characteristic and precision-recall curves, respectively. RMSE and MAE stand for the root-mean-square error and mean absolute error, respectively.

three structural models: our model (referred to as the Full Model), one without *Sharing_type* (DM1; as done in Alagoz et al. 2007a,b),[8] and one without the richness in the waiting cost function (DM2; Alagoz et al. 2004, 2007a,b assume a fixed reward upon waiting, and not as a function of the patient's characteristics). In the category of reduced-form models, we consider three logistic regression models (RM1, RM2, and RM3), with the accept/decline decision as the dependent variable. To make it comparable with the dynamic models, we consider the following independent variables (EC.10 describes the regression estimates). We find that the structural model (Full Model) outperforms all other models in every metric (except MAE, where RM1 and RM2 are better).

$$\textbf{RM1: } d_{it} = a + bGS_{it} + cP(death|MELD_{it}) + \mathbf{d}Sharing\_type_{it} + \mathbf{e}Rec\_age_{it} + fRec\_life\_support_{it} + \mathbf{g}Rec\_med\_cond_{it}$$

$$\textbf{RM2: } d_{it} = a + bGS_{it} + cWait\_time\,(in\ years) + \mathbf{d}Sharing\_type_{it} + \mathbf{e}Rec\_age_{it} + fRec\_life\_support_{it} + \mathbf{g}Rec\_med\_cond_{it}$$

$$\textbf{RM3: } d_{it} = a + \mathbf{b}MELD_{it} + \mathbf{d}Sharing\_type_{it} + \mathbf{e}Rec\_age_{it} + fRec\_life\_support_{it} + \mathbf{g}Rec\_med\_cond_{it}$$

Next, we compare our structural model (Full Model) with LSAM (which is based on 59 parameters). Many studies (Goldberg et al. 2017, Goel et al. 2018) have already pointed out the limitations of LSAM in predicting a patient's offer acceptance behavior in a counterfactual policy. Nevertheless, to illustrate, we consider the Pre-Share 35 and Share 35 policies. The LSAM's probability of acceptance model uses the SRTR's parameter estimates. Our structural model uses the Pre-Share 35 policy era observations to estimate the parameters; and we then use them to predict the probability of offer acceptance in the Share 35 policy era. In Figure 4(a), we plot the average probability of offer acceptance (calculated as a fraction of the offers that were accepted) by the MELD category and use this as a reference. In Figures 4(b) and (c), we plot our structural model's and the LSAM's predicted probabilities of offer acceptance, respectively. Our structural model (in

[8] Although the studies (Alagoz et al. 2007a,b) consider regional and national offers (in terms of their arrival rate), they assume that the reward (or utility) from these offers is the same.

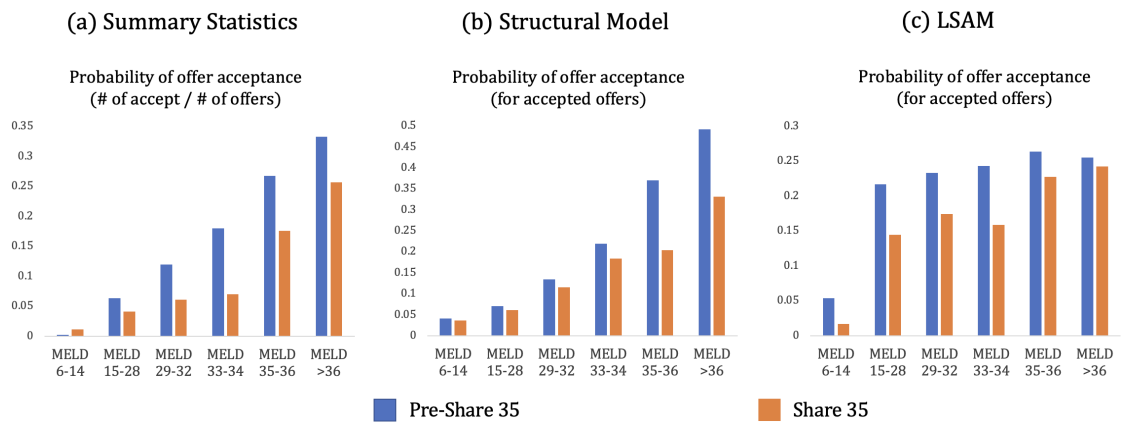

Figure 4 **Out-of-sample comparison of LSAM with dynamic model prediction.**

comparison to LSAM) more accurately captures: (i) the trend of offer acceptance probability (with the MELD category) and (ii) the regime shift (from the Pre-Share 35 to Share 35 policy). EC.10 provides a few more out-of-sample comparisons.

6.6. Comparison of the Pre-Share 35 and Share 35 Policy Eras using the Structural Model

We compare the candidates as a function of their MELD class, region-wise. Given that the probability of an offer acceptance depends on the candidate's state (S_{it}), we weigh the states to come up with a single number for each MELD class and region. For each MELD class (in a region), the weights assigned to the corresponding states (associated with that MELD class) reflect the empirical probabilities (estimated using the data) of being in those states. In Table 8, we report the candidate's offer acceptance probabilities in the Share 35 policy era. Parentheses report the change compared to the Pre-Share 35 policy era.

We see that high-MELD candidates (MELD $\geq$35) in all regions (except region 9) became more selective in the Share 35 policy era, as their acceptance probabilities decreased.[9] Given that the Share 35 policy prioritized sicker candidates in a geographically broader sense, allowing access outside their DSAs, they can afford to be more selective. For lower-MELD classes, we observe heterogeneity (across regions) in their behavioral change. For example, MELD 6-14 candidates experienced a negative effect and became aggressive in more than half of the regions (Regions: 2, 3, 6, 8, 9, 11). It turns out that these regions were associated with a relatively higher organ supply. The average supply (number of deceased donors)-to-demand (number of new patients joining the waiting list) ratio (based on the 2010 to 2018 time period) in these regions was 0.82, compared

[9] Region 9 had the lowest ratio (0.51) of the number of deceased donors to the number of new patients joining the waiting list among all regions (2010 to 2018). It is likely that the Share 35 policy increased competition among the already organ-deficient DSAs (in Region 9), which led to an increase in aggressive behavior in even higher-MELD categories in Region 9 in the Share 35 policy era.

	MELD 6-14	MELD 15-28	MELD 29-32	MELD 33-34	MELD 35-36	MELD >36
Region 1	4% (0%)	4.4% (-0.2%)	7.5% (-0.3%)	13.6% (-0.3%)	22.1% (-1.1%)	33.7% (-1.5%)
Region 2	3.8% (0.1%)	4.1% (-0.1%)	7% (-0.5%)	11% (-1.3%)	14.9% (-4.9%)	23.5% (-7.7%)
Region 3	3.1% (0.2%)	4.5% (0.1%)	6.6% (0.3%)	10.2% (-0.2%)	12.7% (-4.3%)	21.5% (-6.4%)
Region 4	4.6% (-0.2%)	4.7% (-0.6%)	7.7% (-1.3%)	12.9% (-2.6%)	16.9% (-7.1%)	27.2% (-10.2%)
Region 5	3.9% (-0.1%)	4.1% (-0.4%)	6.3% (-0.9%)	10.2% (-1.3%)	15.7% (-3.4%)	25.7% (-7%)
Region 6	4.2% (0.1%)	4.8% (-0.1%)	7.7% (-0.5%)	13.6% (-2.1%)	19.8% (-4.8%)	31.8% (-7.5%)
Region 7	3.6% (-0.1%)	4.1% (-0.5%)	6.8% (-1.1%)	11.9% (-2.3%)	16.5% (-6%)	27.1% (-8.8%)
Region 8	3.7% (0.1%)	4.5% (0%)	7.3% (0.4%)	11.4% (0.5%)	16.7% (-1.4%)	27.1% (-3%)
Region 9	4.6% (0.2%)	4% (0.1%)	6.3% (0.3%)	11% (0.3%)	19.9% (0.8%)	31.5% (1.7%)
Region 10	3.6% (0%)	4.5% (-0.2%)	6.8% (-1%)	9.3% (-2%)	14.5% (-5.7%)	24% (-9.3%)
Region 11	2.9% (0.1%)	4.2% (0%)	6.6% (-0.2%)	10.5% (-0.9%)	14.4% (-5.5%)	23.5% (-8.6%)

Table 8 Offer acceptance probabilities (in the Share 35 policy era) as a function of the MELD category. Parentheses report the change compared to the Pre-Share 35 policy era. Values are calculated using the structural model (whose parameters are estimated using data from 2010 to 2018).

to 0.67 in the rest of the regions. Because the Share 35 policy increased the priority of national patients over low-MELD (<15) local/regional patients, the low-MELD patients in the regions with a higher organ supply became aggressive in response to potentially losing access to organs that were now offered to candidates outside their respective regions.

7. Counterfactual Study

We now discuss the various performance metrics to measure geographic equity and efficiency, as emphasized by HHS (1998), and compare the following policies of interest: (1) Pre-Share 35, (2) Share 35, (3) Acuity Circles, (4) s/d Match, and (5) National Sharing. To delineate the effect of the allocation policy from other factors such as changes in the patient and organ arrival processes, we simulate various policies using common data on patient and organ arrivals. In our simulation setup, we have 5,000 patients and 3,600 donors arriving at different points in time.

Recent studies (Ata et al. 2022, Agarwal et al. 2021) have widely used the iterative simulation approach to estimate the new equilibrium organ offer probabilities in a counterfactual study. Instead of a simulation-based iterative approach, we derive analytical expressions to calculate quantities such as the number of offers, transplants, deaths, and so forth. We use these in an iterative framework (see EC.8 for details, including the simulation setup) to compute the equilibrium organ offer probabilities in an allocation policy. The benefit of using analytical expressions is that it avoids randomness due to the candidates' accept/decline decisions and their MELD transitions, which helps achieve faster convergence with tighter tolerance limits. For performance metrics whose analytical computations are cumbersome, we simulate the organ allocation policy 50 times (using its equilibrium organ offer probabilities) and report the *average*. Performance metrics based on analytical computations are reported as an *expected* quantity.

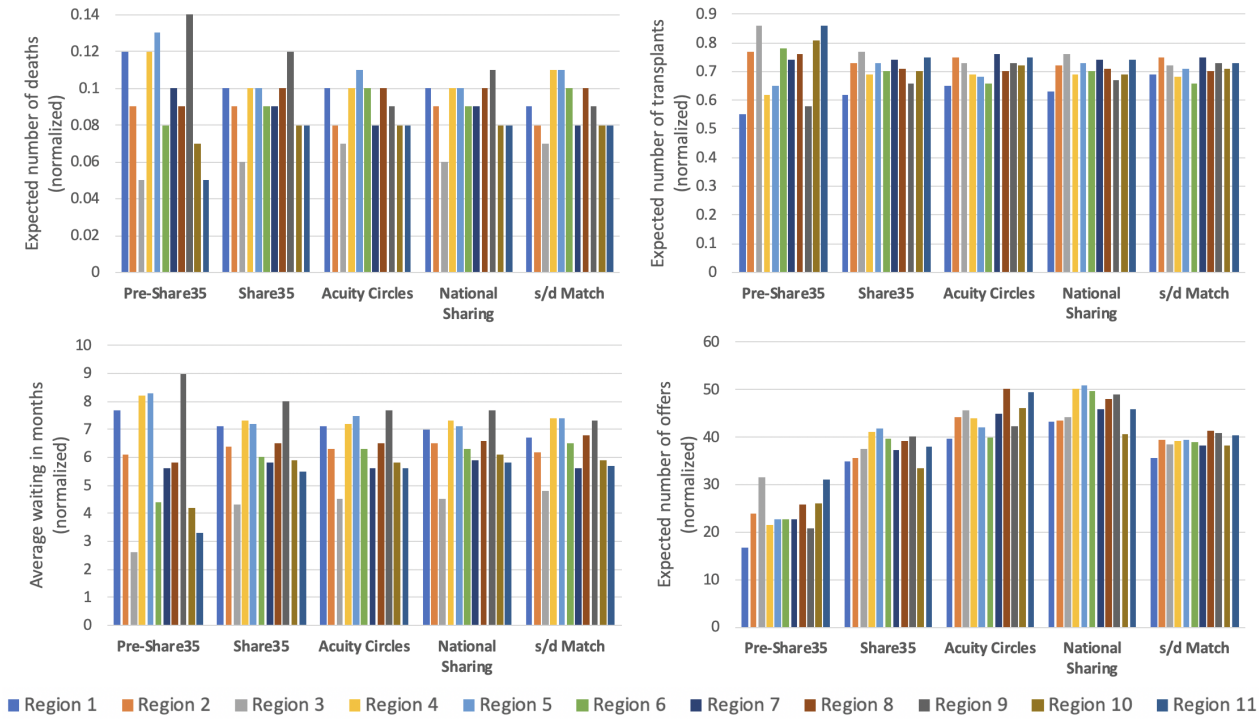

Figure 5 **Comparison of different geographic equity measures between policies.**

7.1. Geographic Equity

Figure 5 compares the expected number of deaths, expected number of transplants, average waiting time in months (that a patient spends on the waiting list until transplantation, death or the end of a simulation), and expected number of offers across regions and between various allocation policies. We report the values after normalizing them with the waiting list volumes in their respective regions. Comparing the Pre-Share 35 and Share 35 policies, we find that the benefit due to the Share 35 policy is higher for regions with lower supply-to-demand ratios in the simulation setup (see EC.11 for details). In Table 9, we report the standard deviations, calculated across regions, for different geographic equity metrics and allocation policies. Compared to the Pre-Share 35 policy, other policies (Share 35, Acuity Circles, National Sharing, and s/d Match) increase geographic equity (as indicated by the decrease in the variability of the performance metrics across regions). The s/d Match (Pre-Share 35) policy has the lowest (highest) variability across all performance measures. Even if we exclude the Pre-Share 35 policy from the comparison, the s/d Match policy has a (0-13)% lower standard deviation (compared to the rest) in the expected number of deaths, (24-35)% less variability in the expected number of transplants, (9-22)% less variability in the average waiting time, and (41-54)% less variability in the expected number of offers.

On an aggregate basis, we find that, out of a total of 5,000 patients in our study, the Pre-Share 35 policy resulted in 499.0 expected deaths; the Share 35 policy resulted in 463.2 deaths;

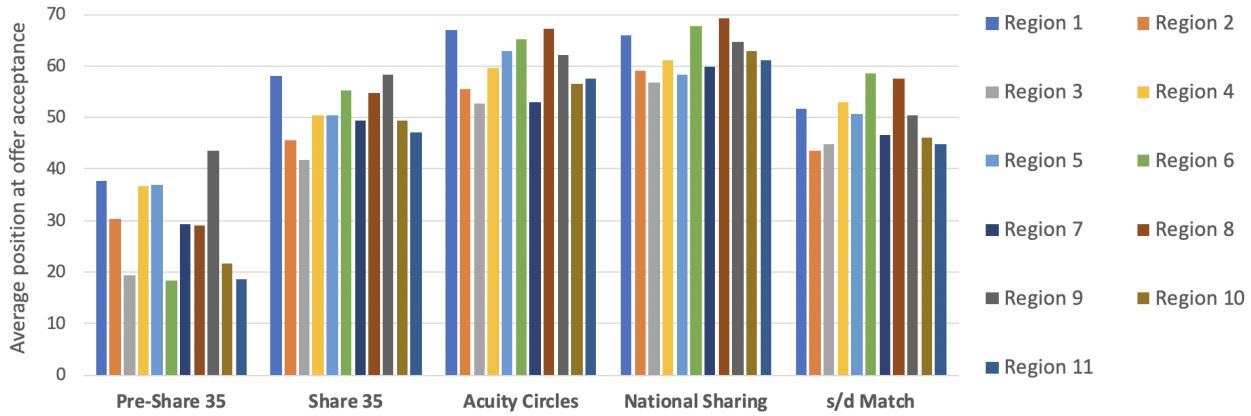

Figure 6 **Comparison of the position at offer acceptance between policies.**

the Acuity Circles policy resulted in 462.2 deaths; the s/d Match policy resulted in 459.9 deaths; and the National Sharing policy resulted in the least number of deaths, 454.1. Out of a total of 3,600 organs, the Pre-Share 35 policy resulted in 3,575.4 expected transplants; the Share 35 policy resulted in 3,570.4 transplants; the Acuity Circles policy resulted in 3,564.3 (lowest) transplants; the s/d Match policy resulted in 3,570.8 transplants; and the National Sharing policy resulted in 3,564.6 transplants.

7.2. Efficiency

We capture efficiency using four performance metrics: position in the queue at offer acceptance, utility derived from transplantation, increase in the patient's survival probability (calculated at the end of one year) due to the transplant, and distance traveled by the organ.

In Figure 6, we compare the average position at which a candidate accepts an offer across regions and between various allocation policies. The three policies (Pre-Share 35, Share 35, and National Sharing) are in increasing order of broader sharing. The Pre-Share 35 policy prioritizes local patients; the Share 35 policy allows more regional and national sharing than its predecessor policy, while the National Sharing policy does not consider geography conditional on the patient's MELD. The Acuity Circles policy can be seen as a broader sharing analogue of the s/d Match policy (given that the latter allows the radius around a donor hospital to be less than 500 NM).

Geographic equity metrics (normalized)	Standard deviation across regions				
	Pre-Share 35	Share 35	Acuity Circles	National Sharing	s/d Match
Deaths	0.031	0.015	**0.013**	0.014	**0.013**
Transplants	0.109	0.043	0.038	0.037	**0.028**
Waiting (in months)	2.164	1.024	0.964	0.878	**0.801**
Offers	4.350	2.626	3.413	3.364	**1.553**

Table 9 **Comparison of the standard deviation of various geographic equity measures between policies. The s/d Match policy has the lowest values for each of the geographic equity metrics.**

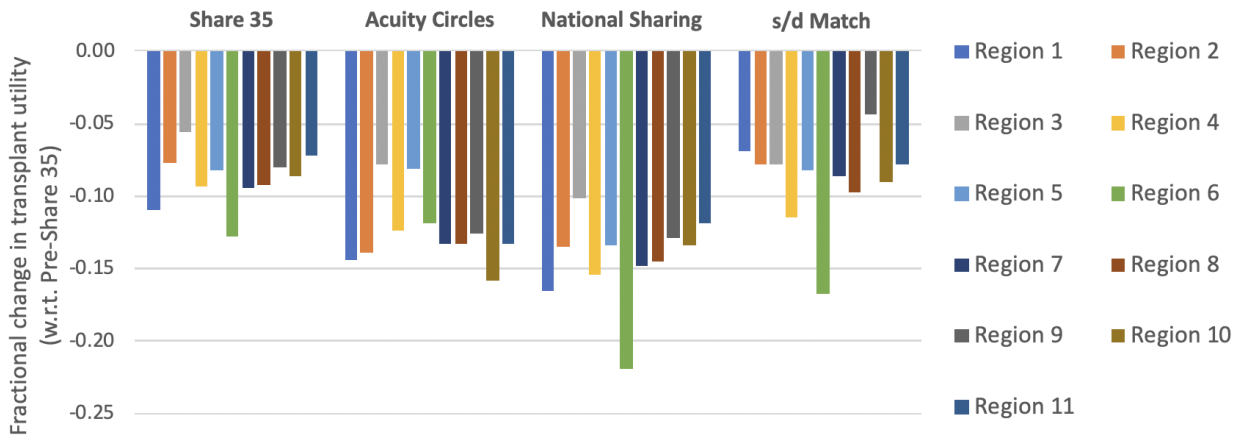

Figure 7 **Comparison of the fractional change in the utility from the transplant (with respect to the Pre-Share 35 policy) between policies.**

We observe that as sharing becomes broader, the position at acceptance and offer refusals increase as a consequence. This is consistent with the takeaway we had drawn (i.e., the Share 35 policy resulted in higher offer refusals) while discussing Figure 3.

Given that utility on its own has no physical interpretation, we report the fractional change in the average utility from transplantation with respect to the Pre-Share 35 policy in Figure 7. We see that all policies are associated with lower transplant utility (as compared to the Pre-Share 35 policy). We also observe that, as the position at the offer acceptance increases, the transplant utility decreases. This is reasonable because offer refusals tend to deteriorate the quality of the organ, and thus, the transplant utility.

Further, we simulate a new policy, Outcome based, where the candidates are sequenced (for organ offers) in decreasing order of the prospective expected utility derived from transplantation. It sets a benchmark for the best outcomes that can be expected for an allocation policy (we note that the Outcome-based policy does not follow the federal guidelines because it does not offer the organ to the sickest patient first). We then estimate the cost of fairness (fractional decrease in the transplant utility with respect to the Outcome-based policy) in Figure 8. The Share 35 and s/d Match policies have the least cost (a 13% decrease in the transplant utility with respect to the Outcome-based policy), while the Acuity Circles and National Sharing policies result in 17% and 19% decrements, respectively.

Next, we calculate the increase in a patient's survival probability due to a transplant as the difference between the probability of graft survival and the probability of a patient's survival without a transplant, both measured at the end of one year. EC.12 provides methodological details. We simulate a new policy, Survival Benefit, where the candidates are sequenced (for organ offers) in decreasing order of the increment in the patient's survival probability due to the transplant. It

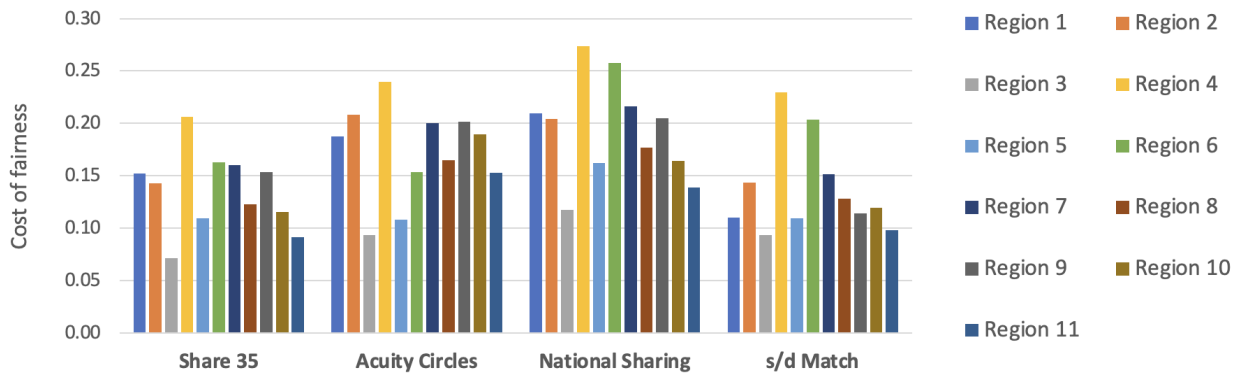

Figure 8 **Cost of fairness for various policies. It is defined as the fractional decrease in the transplant utility with respect to the Outcome-based policy.**

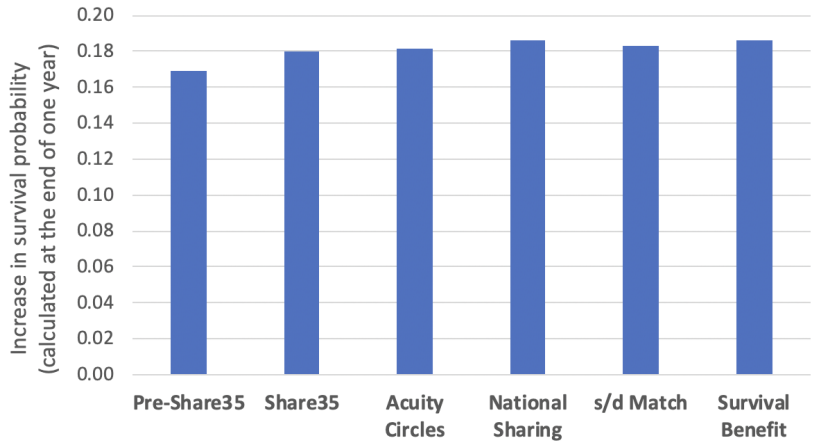

Figure 9 **Comparison of the average increase in the survival probability due to transplantation between policies.**

sets a benchmark for the greatest benefits (in terms of survival probability) that can be expected for an allocation policy (again this policy does not follow the federal guidelines). In Figure 9, we report the average increase in the survival probability due to a transplant in different policy scenarios. We see that the Survival Benefit and National Sharing policies result in the highest benefits (survival probability increases by 0.186 on average), followed by the s/d Match (0.183), Acuity Circles (0.181), Share 35 (0.180), and Pre-Share 35 (0.169) policies. The s/d Match policy is comparable with the benchmark, if not the best.

In Table 10, we compare the travel distance between the policies (we exclude the observations associated with the donor hospitals and transplant centers situated at HIOP (DSA in Hawaii) and PRLL (DSA in Puerto Rico) from the analysis). The distance between any two DSAs' i and j is calculated as the mean of the transplant-volume-weighted distance between the donor hospitals in DSA i and the transplant centers in DSA j, and the reverse. We see that the National Sharing policy results in the largest travel distance, while the Pre-Share 35 policy results in the smallest

	Pre-Share 35	Share 35	Acuity Circles	National Sharing	s/d Match
Mean	240	390	357	503	360
1st quartile	46	59	56	71	52
Median	114	176	197	279	180
3rd quartile	282	528	435	760	417

Table 10 Comparison of the travel distance (in NM) between policies.

travel distance. This is reasonable, given that they are at the two extremes of the broader sharing level. The s/d Match policy is marginally better than the Acuity Circles policy and outperforms the Share 35 policy (in all but the median travel distance).

Overall, the s/d Match policy, which is based on equalizing the s/d ratios by selectively increasing the sharing of donor organs, has the lowest trade-off on the efficiency metrics (compared to the Pre-Share 35 policy) in addressing the issue of geographic inequity. In fact, when a larger radius is allowed around a donor hospital, the s/d ratios are much closer at the transplant centers (i.e., equalized better), and the efficiency metrics are further improved. Please see EC.13 for details. Thus, the s/d Match policy offers a significantly better alternative to the Acuity Circles policy while following the guiding allocation principles laid out by UNOS.

8. Conclusions

We develop a structural model that endogenizes the forward-looking behavior of patients with the allocation policy. We formulate the problem as a discrete-time infinite-horizon dynamic optimization model and use a rich set of patient and donor medical attributes without losing the model's tractability. We compare our dynamic model with LSAM and other reduced-form models to establish the credibility of our structural model, which we use to study counterfactual policies.

First, we study the impact of the Share 35 liver allocation policy (introduced in June 2013) on patients' organ acceptance behavior. We find that the Share 35 policy induced more selective behavior and benefited high-MELD (sicker) patients, with mixed results in low-MELD patients across regions. We also find that the Share 35 policy reduced geographic disparity in metrics such as the number of deaths, access to transplants, waiting time, and organ offers. We observe that the regions with lower supply (deceased donors)-to-demand (new patients) ratios reaped greater benefits. However, the Share 35 policy resulted in more offer refusals and lower average utility from the transplantations.

Recent policies are moving toward broader sharing in principle. The current 'one-size-fits-all' Acuity Circles policy performs very similarly to the Share 35 policy under geographic equity metrics. However, it leads to even lower efficiency (more offer refusals and less utility from transplantation). We illustrate that broader sharing in its current form *is not the best strategy to balance geographic equity and efficiency*. The intuition is that by indiscriminately enlarging the pool of

supply locations from where patients can receive offers, the patients tend to become more selective, resulting in more offer rejections and less efficiency. Instead, a customized approach (equalizing the supply-to-demand ratios across geographies) through the s/d Match policy performs best in addressing the issue of geographic inequity while sacrificing the least efficiency (compared to the Pre-Share 35 policy). This policy selectively enhances the radii around donor hospitals, increasing broader sharing as necessary to equalize the supply and demand. We *strongly recommend that policymakers move away from a 'one-size-fits-all' approach to broader sharing and instead develop broader sharing in a framework that matches the supply and demand*. Such a policy has the greatest potential to score well both in terms of efficiency and geographic equity.

Previous policy proposals have been assessed using LSAM, which uses the same probability acceptance function for candidates and does not consider whether a candidate is residing in an organ-rich/-deficient location. Our study provides a framework for researchers and policymakers to incorporate patients' potential behavioral change into assessing a new policy proposal, which influences their acceptance probability. There is a considerable push in the transplant community to eventually move to a continuous scoring framework. (This framework conceptually gets rid of boundaries. For each organ offer it computes a composite score (used to determine offer sequence) for candidates on the waitlist, which is a combination of factors related to medical priority, the efficiency of organ placement, expected post-transplant outcome, and equity.[10] At this point, the policy parameters (i.e., weights on the different components of the score) are yet to be determined.) An interesting and potentially impactful future study would be to determine the policy parameters in this continuous scoring framework to equalize the s/d ratios across transplant centers.

We limit our study to focus only on geographic inequity (as motivated by prior lawsuits) and do not consider other kinds of disparities such as race, gender, socio-economic factors, organ size, and blood type. Developing a model to incorporate and mitigate these additional disparities is an interesting direction for future research.

Disclaimer: The data reported here have been supplied by the Hennepin Healthcare Research Institute (HHRI) as the contractor for the Scientific Registry of Transplant Recipients (SRTR). The interpretation and reporting of these data are the responsibility of the author(s) and in no way should be seen as an official policy of or interpretation by the SRTR or the U.S. government.

References

Agarwal N, Ashlagi I, Rees M, Somaini P, Waldinger D (2021) Equilibrium allocations under alternative waitlist designs: Evidence from deceased donor kidneys. *Econometrica,* 89(1):37–76.

[10] `https://optn.transplant.hrsa.gov/governance/public-comment/continuous-distribution-of-lungs-concept-paper/`

Akshat S, Gentry SE, Raghavan S (2022) Heterogeneous donor circles for fair liver transplant allocation. *Health Care Management Science* Forthcoming.

Alagoz O, Maillart LM, Schaefer AJ, Roberts MS (2004) The optimal timing of living-donor liver transplantation. *Management Science* 50(10):1420–1430.

Alagoz O, Maillart LM, Schaefer AJ, Roberts MS (2007a) Choosing among living-donor and cadaveric livers. *Management Science* 53(11):1702–1715.

Alagoz O, Maillart LM, Schaefer AJ, Roberts MS (2007b) Determining the acceptance of cadaveric livers using an implicit model of the waiting list. *Operations Research* 55(1):24–36.

Arikan M, Ata B, Friedewald J John, Parker P Rodney (2018) Enhancing kidney supply through geographic sharing in the United States. *Production and Operations Management* 27(12):2103–2121.

Ata B, Friedewald J, Randa AC (2022) Structural estimation of kidney transplant candidates' quality of life scores: Improving national kidney allocation policy under endogenous patient choice and geographical sharing. Working paper, University of Chicago.

Ata B, Skaro A, Tayur S (2017) Organjet: Overcoming geographical disparities in access to deceased donor kidneys in the United States. *Management Science* 63(9):2776–2794.

Atkinson AB (1970) On the measurement of inequality. *Journal of Economic Theory* 2(3):244–263.

Bertsimas D, Farias VF, Trichakis N (2012) On the efficiency-fairness trade-off. *Management Science* 58(12):2234–2250.

Bertsimas D, Farias VF, Trichakis N (2013) Fairness, efficiency, and flexibility in organ allocation for kidney transplantation. *Operations Research* 61(1):73–87.

Bertsimas D, Papalexopoulos T, Trichakis N, Wang Y, Hirose R, Vagefi PA (2020) Balancing efficiency and fairness in liver transplant access: Tradeoff curves for the assessment of organ distribution policies. *Transplantation* 104(5):981–987.

Cox DR (1972) Regression models and life-tables. *Journal of the Royal Statistical Society. Series B (Methodological)* 34(2):187–220.

Demirci MC, Schaefer AJ, Romeijn HE, Roberts MS (2012) An exact method for balancing efficiency and equity in the liver allocation hierarchy. *INFORMS Journal on Computing* 24(2):260–275.

Feng S, Goodrich NP, Bragg-Gresham JL, Dykstra DM, Punch JD, DebRoy MA, Greenstein SM, Merion RM (2006) Characteristics associated with liver graft failure: The concept of a donor risk index. *American Journal of Transplantation* 6:783–790.

Freeman RB, Wiesner RH, Harper A, McDiarmid SV, Lake J, Edwards E, Merion R, Wolfe R, Turcotte J, Teperman L (2002) The new liver allocation system: Moving toward evidence based transplantation policy. *Liver Transplantation* 8(9):851–858.

Garfinkel RS, Nemhauser GL (1970) Optimal political districting by implicit enumeration techniques. *Management Science* 16(8):B495–B508.

Gentry SE, Chow EK, Massie AB, Segev DL (2015) Gerrymandering for justice: Redistricting U.S. liver allocation. *Interfaces* 45(5):462–480.

Gentry SE, Chow EK, Wickliffe CE, Massie AB, Leighton T, Segev DL (2014) Impact of broader sharing on transport time for deceased donor livers. *Liver Transplantation* 20(10):1237–1243.

Goel A, Kim WR, Pyke J, Schladt DP, Kasiske BL, Snyder JJ, Lake JR, Israni AK (2018) Liver simulated allocation modeling: Were the predictions accurate for Share 35? *Transplantation* 102(5):769–774.

Goldberg DS, Levine M, Karp S, Gilroy R, Abt PL (2017) Share 35 changes center level liver acceptance practices. *Liver Transplantation* 23(5):604–613.

Gowrisankaran G, Rysman M (2012) Dynamics of consumer demand for new durable goods. *Journal of Political Economy* 120(6):1173–1219.

Hess SW, Weaver JB, Whelan JN, Zitlau PA (1965) Nonpartisan political redistricting by computer. *Operations Research* 13(6):998–1006.

HHS (1998) Organ procurement and transplantation network; (42 CFR Part 121). *Federal Register* 63(63):16296–16338.

Hughes CB (2015) The history of trying to fix liver allocation: Why a consensus approach will never work. *Clinical Transplant* 29(6):477– 483.

Kilambi V, Mehrotra S (2017) Improving liver allocation using optimized neighborhoods. *Transplantation* 101(2):350–359.

Kim WR, Lake JR, Smith JM, Schladt DP, Skeans MA, Harper AM, Wainright JL, Snyder JJ, Israni AK, Kasiske BL (2018) OPTN/SRTR 2016 Annual data report: Liver. *American Journal of Transplantation* 18, Suppl 1:172–253.

Lee CY, Mangino MJ (2009) Preservation methods for kidney and liver. *Organogenesis* 5(3):105–112.

Rust J (1987) Optimal replacement of GMC bus engines: An empirical model of Harold Zurcher. *Econometrica* 55(5):999–1033.

Schaubel DE, Guidinger MK, Biggins SW, Kalbfleisch JD, Pomfret EA, Sharma P, Merion RM (2009) Survival benefit-based deceased-donor liver allocation. *American Journal of Transplantation* 9:970–981.

Smith JM, Biggins SW, Haselby DG, Kim WR, Wedd J, Lamb K, Thompson B, Segev DL, Gustafson S, Kandaswamy R, Stock PG, Matas AJ, Samana CJ, F SE, Stewart D, Harper A, Edwards E, Snyder JJ, Kasiske BL, Israni AK (2012) Kidney, pancreas and liver allocation and distribution in the United States. *American Journal of Transplantation* 12:3191–3212.

Stahl JE, Kong N, Shechter SM, Schaefer AJ, Roberts MS (2005) A methodological framework for optimally reorganizing liver transplant regions. *Medical Decision Making* 25(1):35–46.

Su X, Zenios SA (2005) Patient choice in kidney allocation: A sequential stochastic assignment model. *Operations Research* 53(3):443–455.

Su X, Zenios SA (2006) Recipient choice can address the efficiency-equity trade-off in kidney transplantation: A mechanism design model. *Management Science* 52(11):1647–1660.

Thompson D, Waisanen L, Wolfe R, Merion RM, Mccullough K, Rodgers A (2004) Simulating the allocation of organs for transplantation. *Health Care Management Science* 7(4):331–338.

Washburn K, Harper A, Timothy B, Edwards E (2016) Changes in liver acceptance patterns after implementation of Share 35. *Liver Transplantation* 22:171–177.

Yeh H, Smoot E, Schoenfeld DA, Markmann JF (2011) Geographic inequity in access to livers for transplantation. *Transplantation* 91(4):479–486.

Zenios SA, Chertow GM, Wein LM (2000) Dynamic allocation of kidneys to candidates on the transplant waiting list. *Operations Research* 48(4):549–569.

Zhang J (2010) The sound of silence: Observational learning in the U.S. kidney market. *Marketing Science* 29(2):315–335.

Electronic Companion

EC.1. Summary Statistics

Table EC.1 reports the summary statistics of various patients, donors, and transplant attributes used in the model. We see that the new patients' age, MELD at listing, and life support status remain almost the same in the Pre-Share 35 and Share 35 policy eras. There is a slight difference in the distribution of the medical condition between the two periods. The donors' age, race distribution, and donation after circulatory death (DCD) status do not change much. However, there is a difference in the cause of death distribution between the two periods. Thus, it is important to control for the donor characteristics in the model. After the Share 35 implementation, on average, offers were accepted later in the queue. Comparing the transplant sharing types, the Share 35 policy resulted in a greater (lower) proportion of regional (local) sharing. Interestingly, the cold ischemia time (CIT), time between organ recovery and transplantation decreased on average (although the coefficient of variation is more than 40%). One might expect the CIT to increase with broader sharing. However, CIT does not follow a linear relationship with distance (due to switching the mode of transport, e.g., from driving to flying for a longer distance). In addition, non-transport factors play a significant role in determining CIT. See Gentry et al. (2014) for a detailed discussion on modeling CIT.

In Figure EC.1, for every MELD class, we plot the mean position at which the candidates in that MELD class received offers. We see a clear dip in offer positions under Share 35 to MELD $\geq$35 candidates, suggesting that patients with a higher MELD were at the top of the offer list. This observation is consistent with what one would expect with the Share 35 policy; organ access increased (decreased) for candidates with a MELD $\geq$35 (MELD $<$35) in general.

Of all the offers, 93.3% were made to the patient-donor pairs of identical blood types, and only 2.4% and 4.3% were made to compatible and incompatible pairs, respectively. Therefore, to keep our model simple and tractable, we do not consider blood type compatibility.

In Table EC.2, we report the candidate's offer acceptance probabilities in the Share 35 policy era, and compare them with the Pre-Share 35 policy era in parantheses. We used a straightforward metric to calculate the acceptance probability (ratio of the number of offers accepted and the number of offers received). We see cases of both an increase and decrease in their acceptance probabilities (e.g., MELD 6-14 in Region 10 saw a 6% increase, whereas MELD 33-34 in Region 6 saw a 26% decrease).

Characteristic	Pre-Share 35 (January 2010-June 2013)	Share 35 (July 2013-December 2018)
Patients		
Age (in years): Mean/SD	54.9/10.3	55.8/11.0
MELD (at listing): Mean/SD	19.3/9.2	19.7/9.8
Life support status:		
Yes	4%	5%
No	96%	95%
Medical condition:		
Intensive care unit (ICU)	8%	3%
Hospitalized	12%	4%
Not hospitalized	80%	93%
Donors		
Age (in years): Mean/SD	44.3/15.2	43.6/14.9
Race:		
White	80%	80%
Black	17%	16%
Others	3%	4%
Cause of death:		
Anoxia	26%	38%
Cerebrovascular accident (CVA)	40%	31%
Others	34%	30%
Donation after circulatory death:		
Yes	13%	17%
No	87%	83%
Fraction of discards	0.252	0.250
Match		
Position at acceptance: Mean/SD	10.6/38.0	15.2/42.5
Cold Ischemia Time (of accepted offers): Mean/SD	6.3/3.0	6.0/2.5
Sharing type (of accepted offers):		
Local	78%	65%
Regional	20%	31%
National	3%	4%

Table EC.1 Summary statistics of patient, donor, and transplant characteristics.

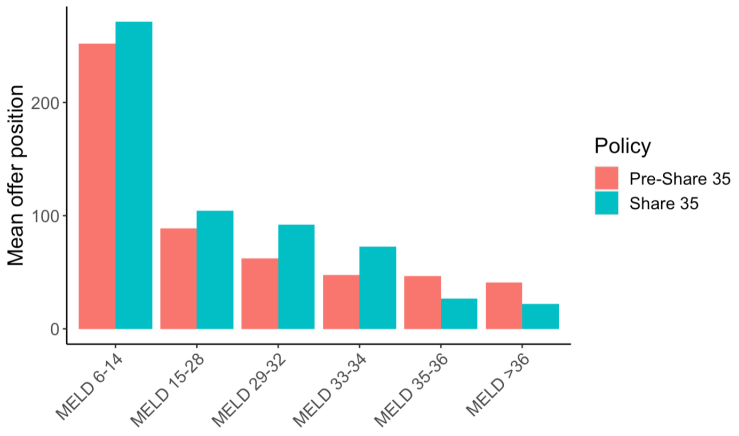

Figure EC.1 Comparison of positions at which offers were made to patients at different MELD scores between policies (Status 1A is assigned a MELD score of 41).

	MELD 6-14	MELD 15-28	MELD 29-32	MELD 33-34	MELD 35-36	MELD >36
Region 1	4.8% (1.5%)	4.5% (-2.8%)	6.1% (-7.6%)	13.9% (-10.4%)	26% (1.5%)	29.5% (-2.3%)
Region 2	1% (0.9%)	2.8% (-1.5%)	8% (-6.1%)	9.1% (-7.8%)	17% (-3%)	22.3% (-3.6%)
Region 3	3.4% (1%)	12.1% (-0.1%)	23.6% (-11.1%)	26.4% (-15%)	37.6% (1.9%)	36.9% (-8.6%)
Region 4	0.7% (0.4%)	2.5% (-4.3%)	9.2% (-18%)	16.8% (-21.3%)	25% (-11.7%)	32% (-4.9%)
Region 5	1.2% (0.9%)	2.1% (-0.8%)	3.4% (-7.3%)	5.1% (-10.9%)	10.9% (-13.4%)	23.7% (-9%)
Region 6	0% (0%)	6.1% (-6.3%)	14.9% (-17.7%)	20.4% (-25.9%)	27.2% (-24.8%)	28.6% (-17.1%)
Region 7	1% (-0.3%)	3.4% (-6.4%)	9.7% (-9.9%)	14.5% (-14%)	22.4% (-10.5%)	27.8% (-8.9%)
Region 8	0.5% (0.2%)	7.5% (-2.1%)	16.8% (-19.6%)	20.8% (-19.3%)	34.5% (4.2%)	38.3% (-3.4%)
Region 9	0.9% (0.8%)	1.4% (-0.3%)	2.6% (-5.1%)	6.4% (-9.6%)	14.1% (-6.9%)	25.6% (-11%)
Region 10	8.3% (6.2%)	10.7% (-5.2%)	20.6% (-12.9%)	20.3% (-10.6%)	34.6% (-8.5%)	40.3% (0.6%)
Region 11	1.5% (1.3%)	8.7% (-5.2%)	21.4% (-18%)	24.6% (-15.9%)	42.4% (-6.2%)	45% (0.8%)

Table EC.2 Offer acceptance probabilities (in the Share 35 policy era) as a function of the MELD category. Parentheses report the change, compared to the Pre-Share 35 policy era. Values are calculated using summary statistics.

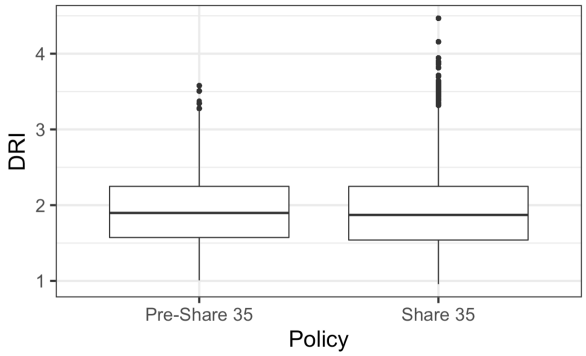

Figure EC.2 Comparison of the organ quality of declined offers between the Pre-Share 35 and Share 35 policy eras using the donor risk index (DRI).

EC.2. Comparing the Organ Quality of Declined Offers

We use the metric, the donor risk index (DRI), proposed by Feng et al. (2006) to evaluate the quality of declined offers. This index measures the quality of an organ using demographic factors (age, race, height), cause and type of donor death, sharing type (local/regional/national), and CIT. A higher DRI is associated with a greater risk of graft failure. Because CIT is observed only for accepted offers, we use the median value (=6.9 hours) in our calculation. In Figure EC.2, we compare the box plots of the DRI between the Pre-Share 35 and Share 35 policy eras. We see that there are no significant differences in the distributions of organ quality.

EC.3. Details on Logit Inclusive Value

In a dynamic model, agents (patients, in our case) have perceptions over future states. They need to know the evolution of every element in the state space. If the number of elements is large, it can

make the model very complex. To make the problem tractable, a simplifying assumption is often made: the evolution of the space space is approximated using a lower dimensional Markov process (see Gowrisankaran and Rysman 2012). In other words, agents are considered boundedly rational, and they use fewer elements to form predictions about the future.

In our context, the graft survival probability is calculated using the SRTR Risk Adjustment Model,[11] which is based on a total of 41 predictors (Z_{it}) that include the candidate's and donor's medical attributes, and CIT. Including all the 41 predictors in the state space will result in a curse of dimensionality. Following the extant literature (Gowrisankaran and Rysman 2012) on the *logit inclusive value*, we simplify the evolution of those 41 medical attributes using the evolution of one-dimensional GS_{it}.

We model GS_{it} as a function of the MELD category ($MELD_{it}$), age group (Rec_age_{it}), life support status ($Rec\_life\_support_{it}$), medical condition ($Rec\_med\_cond_{it}$), and organ type (Q_{it}). For every combination of the (values taken by the) above variables, we first filter the offers. For this subset of offers, we observe the values of all the 41 predictors,[12] and we calculate the graft survival probability (using the SRTR Risk Adjustment Model) for each offer. The average of the graft survival probabilities is the value of GS_{it}. In other words, we group the offers by $(MELD_{it}, Rec\_age_{it}, Rec\_life\_support_{it}, Rec\_med\_cond_{it}, Q_{it})$, and GS_{it} is the average of the graft survival probabilities for these offers. Thus, GS_{it} is always $\leq$1. In this way, we approximate the evolution of 41-dimensional Z_{it} with the evolution of GS_{it}, which is one-dimensional. As a sanity check, we regress GS_{it} with the MELD category, age group, life support status, medical condition, and organ type in Table EC.4. We find that the signs and the relative ordering of the regression estimates are reasonable.

EC.4. State Transition Probability

A patient's health condition evolves stochastically and is a major determinant of her priority in a queue in the organ allocation policies studied. The state transition probability is written as:

$$\begin{aligned}\mathcal{P}(S_{i,t+1}|S_{it}, d_{it}=0) = \mathcal{P}(&MELD_{i,t+1}, Rec\_age_{i,t+1}, Rec\_life\_support_{i,t+1}, Rec\_med\_cond_{i,t+1},\\ &Q_{i,t+1}, Z_{i,t+1}, Sharing\_type_{i,t+1}|MELD_{it}, Rec\_age_{it}, Rec\_life\_support_{it},\\ &Rec\_med\_cond_{it}, Q_{it}, Z_{it}, Sharing\_type_{it}, d_{it}=0)\end{aligned} \tag{EC.1}$$

Because the priority of a candidate on the offer list does not depend on past offers, by dropping the history of the previous period's offer, the transition probability can be rewritten as:

[11] `https://www.srtr.org/reports-tools/posttransplant-outcomes/` accessed on July 12, 2020.

[12] We use a constant value of CIT (=6.9 hours) in our model. We do not consider GS_{it} to depend on $Sharing\_type_{it}$.

	MELD class						
	MELD 6-14	MELD 15-28	MELD 29-32	MELD 33-34	MELD 35-36	MELD >36	Death
MELD 6-14	0.9958	0.0036	0.0002	0.0001	0.0000	0.0000	0.0003
MELD 15-28	0.0049	0.9922	0.0016	0.0002	0.0001	0.0002	0.0008
MELD 29-32	0.0041	0.0120	0.9693	0.0082	0.0022	0.0020	0.0021
MELD 33-34	0.0042	0.0070	0.0092	0.9508	0.0166	0.0086	0.0036
MELD 35-36	0.0062	0.0112	0.0114	0.0114	0.8809	0.0688	0.0102
MELD >36	0.0098	0.0123	0.0051	0.0036	0.0059	0.9335	0.0299
Death	0	0	0	0	0	0	1

Table EC.3 MELD transition matrix.

$$\mathcal{P}(S_{i,t+1}|S_{it}, d_{it}=0) = \mathcal{P}(MELD_{i,t+1}, Rec\_age_{i,t+1}, Rec\_life\_support_{i,t+1}, Rec\_med\_cond_{i,t+1},$$
$$Q_{i,t+1}, Z_{i,t+1}, Sharing\_type_{i,t+1}|MELD_{it}, Rec\_age_{it}, Rec\_life\_support_{it},$$
$$Rec\_med\_cond_{it}, Z_{it}, d_{it}=0) \tag{EC.2}$$

We assume that the MELD state transition is the same for all age groups, life support statuses, and medical conditions (the pooling of various patient types enables the estimation of the MELD state transition matrix with greater confidence than estimating multiple (18 in our case, see Section 6.2) matrices for different patient types). *Death* is an absorbing state. Next, when an organ arrives, the allocation policy does not depend on the candidate's age, life support status, or medical condition. Thus, only MELD plays a role in determining the organ offer probabilities, $\mathcal{P}(Q)$, in a policy. These allow us to simplify the transition probability as:

$$\mathcal{P}(S_{i,t+1}|S_{it}, d_{it}=0) = \mathcal{P}(MELD_{i,t+1}|MELD_{it}, d_{it}=0) \times \mathcal{P}(Q_{i,t+1}|MELD_{i,t+1}, d_{it}=0) \times$$
$$\mathcal{P}(Rec\_age_{i,t+1}, Rec\_life\_support_{i,t+1}, Rec\_med\_cond_{i,t+1}, Z_{i,t+1}, Sharing\_type_{i,t+1}|$$
$$MELD_{i,t+1}, Q_{i,t+1}, MELD_{it}, Rec\_age_{it}, Rec\_life\_support_{it}, Rec\_med\_cond_{it}, Z_{it}, d_{it}=0) \tag{EC.3}$$

We estimate $\mathcal{P}(MELD_{i,t+1}|MELD_{it}, d_{it}=0)$ from the data (January 2003 to February 2019) on MELD transitions (Table EC.3). To estimate $\mathcal{P}(Q_{i,t+1}|MELD_{i,t+1}, d_{it}=0)$, we adopt an approach identical to Alagoz et al. (2007b):

$$\mathcal{P}(Q_{i,t+1}|MELD_{i,t+1}, d_{it}=0) = \frac{\sum_i \#\text{ of offers of type } Q_{i,t+1} \text{ candidate } i \text{ received at } MELD_{i,t+1}}{\sum_i \#\text{ of days candidate } i \text{ waited at } MELD_{i,t+1}} \tag{EC.4}$$

It is possible that a candidate does not receive an offer on a given day. We add *no_offer* to Q_{it} (calculated as per equation EC.4) and $Sharing\_type_{it}$ (if $Q_{it} = no\_offer$, $Sharing\_type_{it}$=*no_offer*, and vice versa).

Now, we are left with modeling the evolution of $Sharing\_type_{it}$, Z_{it}, Rec_age_{it}, $Rec\_life\_support_{it}$, and $Rec\_med\_cond_{it}$. The *Sharing_type* depends on the candidate's MELD and organ characteristics. Low-quality organs are usually declined more often and are likely to be shared nationally. Sicker patients get higher priority; therefore, they are likely to receive local/regional offers

more often. Thus, we model the transition of $Sharing\_type_{it}$ as in equation EC.6. Next, Z_{it} consists of 41 predictors, each of which takes a set of values. Including them in the structural model will cause a state space explosion and impede the transition probability matrix estimation. We use the *logit inclusive value* technique to simplify the evolution of 41 predictors using the transition of one-dimensional GS_{it} (see EC.3). We replace Z_{it} with GS_{it} in the state transtion probability expression (equation EC.5). A patient predicts the value of $GS_{i,t+1}$ using $(MELD_{i,t+1}, Rec\_age_{i,t+1}, Rec\_life\_support_{i,t+1}, Rec\_med\_cond_{i,t+1}, Q_{i,t+1})$. Next, the data do not include the patient's transition of life support or medical condition. Only the MELD of the patient evolves over time. Patients differing in age group, life support status, and medical condition can be thought of as different patient types. These assumptions allow us to simplify the transition probability to:

$$\begin{aligned}\mathcal{P}(S_{i,t+1}|S_{it}, d_{it}=0) = \mathcal{P}(MELD_{i,t+1}|MELD_{it}, d_{it}=0) \times \mathcal{P}(Q_{i,t+1}|MELD_{i,t+1}, d_{it}=0)\times \\ \mathcal{P}(GS_{i,t+1}|MELD_{i,t+1}, Rec\_age_{i,t+1}, Rec\_life\_support_{i,t+1}, Rec\_med\_cond_{i,t+1}, Q_{i,t+1}, d_{it}=0)\times \\ \mathcal{P}(Sharing\_type_{i,t+1}|MELD_{i,t+1}, Q_{i,t+1}, d_{it}=0)\times \\ \mathbb{1}_{\{Rec\_age_{i,t+1}=Rec\_age_{it}, Rec\_life\_support_{i,t+1}=Rec\_life\_support_{it}, Rec\_med\_cond_{i,t+1}=Rec\_med\_cond_{it}\}}, \end{aligned} \tag{EC.5}$$

where $\mathcal{P}(Sharing\_type_{i,t+1}|MELD_{i,t+1}, Q_{i,t+1}, d_{it}=0)$ is estimated as:

$$\frac{\sum_i \#\text{ of offers of type } Q_{i,t+1} \text{ received at } MELD_{i,t+1} \text{ that have } Sharing\_type_{i,t+1}}{\sum_i \#\text{ of offers of type } Q_{i,t+1} \text{ received at } MELD_{i,t+1}} \tag{EC.6}$$

The MELD transition matrix and GS_{it} are estimated based on the data of the entire U.S. However, the estimation of $\mathcal{P}(Q_{i,t+1}|MELD_{i,t+1}, d_{it}=0)$ and $\mathcal{P}(Sharing\_type_{i,t+1}|MELD_{i,t+1}, Q_{i,t+1}, d_{it}=0)$ are done for every DSA-policy era pair separately (while evaluating a policy that uses TC instead of DSA, we estimate the quantities for every TC). This is because the organ offer and sharing-type probabilities might differ across the DSAs and, in the Pre-Share 35 and Share 35 policy eras.

EC.5. Log-Likelihood Function

When an offer is made, the probability of accepting an offer, equation (6), can be rewritten as:

$$P(d_{it}=1|S_{it}) = \frac{e^{EU(S_{it})}}{e^{EU(S_{it})} + e^{-EW(S_{it})+\delta EV(S_{it})}}, \tag{EC.7}$$

Taking the log of both sides,

$$\ln\left(P(d_{it}=1|S_{it})\right) = \ln\left[e^{EU(S_{it})}\right] - \ln\left[e^{EU(S_{it})} + e^{-EW(S_{it})+\delta EV(S_{it})}\right] \tag{EC.8}$$

$$\text{Also,} \qquad \ln\left(P(d_{it}=0|S_{it})\right) = \ln\left[e^{-EW(S_{it})+\delta EV(S_{it})}\right] - \ln\left[e^{EU(S_{it})} + e^{-EW(S_{it})+\delta EV(S_{it})}\right] \tag{EC.9}$$

The log-likelihood of a candidate's observed decision is:

$$\{\ln\left(P(d_{it}=1|S_{it})\right)\}^{d_{it}} \times \{\ln\left(P(d_{it}=0|S_{it})\right)\}^{(1-d_{it})} \tag{EC.10}$$

Grouping over all patients' decisions, the log-likelihood function is:

$$\begin{aligned}
&\sum_{i,t}\left(\mathbb{1}_{\{d_{it}=1\}}\ln\left(P\left(d_{it}=1|S_{it}\right)\right)+\mathbb{1}_{\{d_{it}=0\}}\ln\left(P\left(d_{it}=0|S_{it}\right)\right)\right)\\
&=\sum_{S_{it}}\left(n_{accept}^{S_{it}}\ln\left(P\left(d_{it}=1|S_{it}\right)\right)+n_{decline}^{S_{it}}\ln\left(P\left(d_{it}=0|S_{it}\right)\right)\right)\\
&=\sum_{S_{it}}n_{accept}^{S_{it}}\left(EU(S_{it})-ln[e^{EU(S_{it})}+e^{-EW(S_{it})+\delta EV(S_{it})}]\right)+\\
&n_{decline}^{S_{it}}\left(-EW(S_{it})+\delta EV(S_{it})-ln[e^{EU(S_{it})}+e^{-EW(S_{it})+\delta EV(S_{it})}]\right)\\
&=\sum_{S_{it}}n_{accept}^{S_{it}}EU(S_{it})+n_{decline}^{S_{it}}(-EW(S_{it})+\delta EV(S_{it}))-\\
&\left(n_{accept}^{S_{it}}+n_{decline}^{S_{it}}\right)\times(ln[e^{EU(S_{it})}+e^{-EW(S_{it})+\delta EV(S_{it})}])
\end{aligned} \tag{EC.11}$$

Every candidate i has an associated state S_{it} at time t; therefore, we can sum over the elements in the state space, accounting for the number of candidates in those states (instead of summing over the candidates and time periods when they made the decisions). The first equality follows from this fact, where $n_{accept}^{S_{it}}$ and $n_{decline}^{S_{it}}$ denote the number of candidates who accepted and declined the offers in state S_{it}, respectively.

EC.6. Details on Identification of β_{GS}

We want to check whether the variables (on which we rely to identify GS_{it}, and whose variation we observe in the data) are correlated with GS_{it} or not. In Table EC.4, we regress GS_{it} with the MELD category, age group, life support status, medical condition, and organ type. We find that most of the regression estimates are statistically significant, and 55% of the variability in GS_{it} is explained by the independent variables used in the regression. Thus, we can identify GS_{it} in the structural model through the variation of these independent variables in the observed data.

EC.7. Relaxing the Assumption of a Fixed Value of CIT

In our main model, we assumed a fixed value of CIT and endogenized *sharing_type* (which captured the effect of CIT) with the allocation policy. As a robustness check, we relax the assumption and build a CIT prediction model (a linear regression model). We need a prediction model because CIT is only observed for accepted offers, and not for declined offers. We then used the predicted CIT values (instead of a fixed value of 6.9 hours) in calculating the one-year graft survival probability. In Table EC.5, we compare the structural model estimates (when we use fixed CIT versus the predicted CIT). We find that there's only a slight change in the estimates of the utility and

Independent variable	Estimate
Intercept	0.9582***
MELD 15-28	0.0028
MELD 29-32	-0.0058*
MELD 33-34	-0.008**
MELD 35-36	-0.0127***
MELD >36	-0.0203***
Candidate age group: R2 (45-65 years)	-0.0211***
Candidate age group: R3 (≥65 years)	-0.0268***
Candidate life support: Yes	-0.0492***
Candidate medical condition: H	-0.0182***
Candidate medical condition: ICU	-0.0649***
Donor controls: Yes	
No. of parameters: 58	
(Adjusted) R-squared = (0.5438) 0.5518	
No. of observations = 3,264	

$^{***}p < 0.001$; $^{**}p < 0.01$; $^{*}p < 0.05$

Table EC.4 Estimation results of regressing GS.

waiting cost functions parameters. The estimates of the parameters associated with regional and national sharing are closer to zero in the predicted CIT model than the fixed CIT model. This is because some of the disutilities (associated with regional/national sharing) are captured by the higher CIT in the predicted CIT model. Although the log-likelihood value is slightly better in the latter case, we prefer to use the fixed CIT model in our main analysis due to the following reasons: (1) Nonavailability of the key variables (mode of organ transport) for predicting CIT; (2) In counterfactual studies, we would need to predict CIT. Because we are less confident in the CIT prediction model, the prediction inaccuracies will make the policy evaluation less reliable; and (3) The measurement error in CIT (due to using a predicted value) will be passed over to the structural model.

EC.8. Iterative Method for Estimating the Equilibrium

We simulate different organ allocation policies. The common inputs across the policies are the sampled organ and candidate arrivals, the MELD transition matrix, and the estimates from the structural model. We randomly sample 5,000 patients and 3,600 donors from the 11 regions, which arrive at different points in time ($t = 1, ..., 730$). Every organ is offered to a maximum of 500 candidates (which is close to the 99^{th} percentile in the actual dataset) before being discarded. We let 34% of the patients be on the waiting list at $t = 1$, and the initial MELD distribution of the patients is chosen so that they represent the actual data. We consider two patient groups ($\{$(*Rec_age*:<45 years, *Rec_life_support*='No', *Rec_med_cond*='NH') and (*Rec_age*: $(45-65)$ years, *Rec_life_support*='No', *Rec_med_cond*='NH')$\}$, which constitutes 83% of the patient population in the UNOS data) and 48 organ types in the simulation study. Various patient groups may have different probabilities of acceptance for the same organ due to differences in the expected utilities

Variable	Parameter	Fixed CIT Estimate (SE)	Predicted CIT Estimate (SE)
Utility Function:			
Intercept	β_0	-21.7803 (0.3145)	-22.5536 (0.3257)
Sharing type: Regional	$\beta_{Sharing}$	-1.0348 (0.0113)	-0.9655 (0.0114)
Sharing type: National		-2.3328 (0.0243)	-2.0680 (0.0247)
Graft survival probability (GS)	β_{GS}	19.5200 (0.3353)	20.3111 (0.3468)
Waiting Cost Function:			
Death	ω_d	0.1160 (0.0007)	0.1153 (0.0007)
Candidate age group: R2 (45-65 years)	ω_{Age}	0.0057 (0.0002)	0.0058 (0.0002)
Candidate age group: R3 ($\geq$65 years)		0.0061 (0.0003)	0.0063 (0.0003)
Candidate life support: Yes	ω_{LS}	0.0134 (0.0008)	0.0130 (0.0008)
Candidate medical condition: H	ω_{MC}	0.0114 (0.0004)	0.0115 (0.0004)
Candidate medical condition: ICU		0.0229 (0.0008)	0.0232 (0.0008)
No. of observations		890,402	890,402
Log-likelihood		-173,630.9	-173,579.2

Table EC.5 Comparison of the estimation results of the structural models (when CIT is fixed versus predicted).

(derived from the transplant) and waiting costs. The equilibrium behavior of each group will depend on the presence of the others; further, by considering two groups in our study, we capture their interactions in the equilibrium offer acceptance probabilities. The steps (followed by the pseudo algorithm) to estimate the steady-state equilibrium (for each allocation policy) using the iterative method are given below:

1. Start with the organ offer and sharing-type probabilities: $\mathcal{P}^{(k)}(Q_{it}|MELD_{it})$ and $\mathcal{P}^{(k)}(Sharing\_type_{it}|MELD_{it}, Q_{it})$. This enables us to calculate the state transition matrix, $\Pi^{(k)}$. Using the 'inner' algorithm of the nested fixed point algorithm, estimate $EV^{(k)}(.)$. When $k=0$, we start with arbitrary values of the above quantities. Skip the next step if $k=0$.

2. If $||EV^{(k)}(.) - EV^{(k-1)}(.)||_\infty < \varepsilon_1$, stop, or else go to the next step. We use $\varepsilon_1 = 10^{-5}$.

3. Calculate the probability of acceptance: $P^{(k)}(d_{it}=1|S_{it}) = \frac{e^{EU(S_{it})}}{e^{EU(S_{it})}+e^{-EW(S_{it})+\delta EV^{(k)}(S_{it})}}$.

4. Policy simulation: For an allocation policy, we analytically calculate the expected number of offers, expected number of transplants, and expected waiting period by any time t. Using analytical expressions avoids the randomness introduced due to candidates' accept/decline decisions and their MELD transitions, which helps achieve faster convergence with tighter tolerance limits. First, we create a table of states for every geography (DSA or TC) and tabulate the patient counts in those states. Each state has its own probability of acceptance. A patient's state might transition to other states (the patient's geography does not change). At different points in time, new patients join the waiting list, and donors arrive; some patients receive offers, get a transplant, and leave the system. To analytically calculate the expected number of offers received and transplants (to patients in various MELD classes and geographies) due to an organ arriving at time t, we sum the finite geometric series sequentially in the order (determined by the allocation policy) in which the

offers are made to the various patient groups. The patients who received transplants are removed from the waiting list. Using the MELD transition matrix, we calculate the expected number of patients transitioning to different MELD categories at time $t+1$ and update the waiting list. New patients who join the waiting list at time $t+1$ are added. If no donor arrives at time $t+1$, only the MELD transitions occur. We can track the expected number of patients on the waiting list, number of offers received, and number of transplants at different instances of t. This enables us to calculate the quantities of interest to us, which are the organ offer and sharing-type probabilities: $\mathcal{P}^{(k)}(Q_{it}|MELD_{it})$ and $\mathcal{P}^{(k)}(Sharing\_type_{it}|MELD_{it},Q_{it})$ in the k^{th} step of the iterative method.

5. Update k to $k+1$. Go to Step 1.

Each iteration took approximately 25 hours for policies using the TC as the geographic unit (and approximately nine hours for DSA-based policies), and we were able to achieve convergence within 10 iterations for every policy. For the Acuity Circles policy, we define 'local' sharing if the distance between the donor hospital and the TC is <66 NM (average of the distance between the donor hospital and TC pairs in the same DSA), 'regional' sharing if the distance is ≥66 NM and <262 NM (average of the distance between the donor hospital and TC pairs in the same region), and 'national' otherwise.

Algorithm 1 Steady State Equilibrium

Input: Candidate and organ characteristics, allocation policy, structural parameters (β_0, β_{GS}, $\beta_{Sharing}, \omega_d, \omega_{Age}, \omega_{LS}, \omega_{MC}$), MELD transition matrix. Let t be the arrival time of an organ.

Output: $EV^*(S_{it}), \mathcal{P}^*(Q_{it}|MELD_{it}), \mathcal{P}^*(Sharing\_type_{it}|MELD_{it},Q_{it})$.

Initialize k=0 and beliefs $EV^k(S_{it}), \mathcal{P}^k(Q_{it}|MELD_{it})$, and $\mathcal{P}^k(Sharing\_type_{it}|MELD_{it},Q_{it})$ for all possible values of $S_{it}, Q_{it}, MELD_{it}$ and $Sharing\_type_{it}$.

repeat

  $\Pi^k \leftarrow$ Compute state transition matrix (see equation EC.5)

  Initialize $m=0$ and $EV^m(.)$

  repeat

    $EV^m(.) \leftarrow \Pi^k \times \ln\left[e^{EU(.)} + e^{-EW(.)+\delta EV^m(.)}\right]$

    $m \leftarrow m+1$

  until $m \geq 1, \left\|EV^m(.) - \Pi \times \ln\left[e^{EU(.)} + e^{-EW(.)+\delta EV^m(.)}\right]\right\|_\infty < 10^{-9}$;

  $EV^k(.) \leftarrow EV^m(.)$

  $p^k_{acpt}(S_{it}) := P^k(d_{it}=1|S_{it}) \leftarrow$ Compute offer acceptance probabilities $\forall S_{it}$ (see equation EC.7)

  $\mathcal{P}^k(Q_{it}|MELD_{it}), \mathcal{P}^k(Sharing\_type_{it}|MELD_{it},Q_{it}) \leftarrow$ Policy Simulation $(p^k_{acpt}(.))$

  $k \leftarrow k+1$

until $k>1, \left\|EV^k(.) - EV^{k-1}(.)\right\|_\infty < 10^{-5}$;

$EV^*(S_{it}) \leftarrow EV^k(S_{it}), \mathcal{P}^*(Q_{it}|MELD_{it}) \leftarrow \mathcal{P}^k(Q_{it}|MELD_{it})$,

$\mathcal{P}^*(Sharing\_type_{it}|MELD_{it},Q_{it}) \leftarrow \mathcal{P}^k(Sharing\_type_{it}|MELD_{it},Q_{it})$

EC.9. Numerical Study to Derive Insights from the Structural Model

The allocation policies essentially differ in the utility of waiting or the future prospects of being offered an organ (through the expected future value, $EV(S_{it})$). The objective of this exercise is to generate insights about how a patient would react to the possibility of a transplant based on her health status and her future prospect of being offered an organ. This, in turn, depends on the organ offer probability, which depends on the supply and demand at the various DSAs and the allocation policy in place. For this reason, we study the effect of a change in supply and demand on a patient's organ acceptance behavior.

Setup

We simulate the organ and candidate arrivals for a two-year time period ($t = 1, ..., 730$). We use a stylized setup of two regions and three DSAs (Region A: DSA 1 and DSA 2; Region B: DSA 3), each with a single TC, in our numerical study. We let 34% of the patients be on the waiting list at $t = 1$, and the initial MELD distribution of the patients is chosen so that they represent the actual data. We only consider a single patient type (*Rec_age*: $(45-65)$ years, *Rec_life_support*='No', *Rec_med_cond*='NH'), and a single organ type (*Don_age*: $(18-39)$ years, *Don_race* = 'White', *Don_cod* = 'Others', *Don_dcd* = 'No'). They represent the most frequent patient and organ types.

We study a total of five settings of demand and supply across the DSAs (Set 1,..., Set 5; see Table 6). The organ and the candidate's arrival times are random; we run 20 iterations for each setting. The steady state equilibrium organ acceptance probabilities are estimated using Algorithm 1 in EC.8. We consider two organ allocation policies: Share 35 and the Acuity Circles. The insights, as we will see, remain the same.

Discussion of Insights

In Table 6, we report the probability of offer acceptance (95% confidence interval) as a function of a patient's MELD category and DSA. We select Set 1 as the baseline scenario: a similar supply and demand volume (in aggregate) is there at Region A and Region B, and at DSA 1 and DSA 2. We then change either the demand or s/d ratio, one at a time. We conduct an intra-set analysis (discuss the results of each set on its own), and an inter-set analysis (compare a set with the baseline setting, Set 1). Before we proceed, it is useful to do a quick sanity check. The two DSAs in Region A have similar characteristics in Set 1, Set 3 and Set 5. Therefore, the probability of offer acceptance should also be the same for a patient in DSA 1 and DSA 2 (for a given MELD category and a given set). Our results are consistent with our expectation, i.e., the confidence intervals overlap. We note that there are more observations for lower-MELD categories; therefore, the confidence interval is smaller for lower-MELD categories.

Set 1 (baseline setting): The aggregate s/d ratio is the same for Regions A and B. One may expect that the probability of offer acceptance should also be the same. However, sharing within

Region B is all local, whereas sharing within Region A will be a mix of local and regional. Therefore, the behavior of Region B patients might be different from their counterparts in Region A.

We find that DSA 3 patients are more selective than DSA 1 and 2 patients. This selective nature is more prominent in middle-MELD categories (such as MELD 29-34). For a lower-MELD patient to receive an organ offer, it has to be declined by the higher-MELD patients of both the regions. Thus, we do not see a significant difference between the organ acceptance probabilities between the two regions in lower-MELD patients. Higher-MELD (MELD ≥ 35) patients do not have significant difference in organ access, in this stylized model, due to broader sharing under both the Share 35 and Acuity Circles policies.

Set 2 (and its comparison with Set 1): In Set 2, we decrease the supply at DSA 2 such that the new s/d ratio in DSA 2 becomes 0.5 (from 0.7). The DSA 2 patients have a higher probability of offer acceptance than DSA 1 patients due to lesser organ access. This aggressive behavior is especially at lower MELD scores (the impact of difference in the s/d ratio is attenuated at higher MELD scores due to the prioritization of higher-MELD patients through broader sharing).

Upon comparing with Set 1, we see that DSA 2 patients react by increasing their probability of offer acceptance (especially at MELD 6-32). We also observe that a decrease in supply at DSA 2 affects other DSAs as well. DSA 1 patients became aggressive (than Set 1), especially at MELD 6-28. DSA 3 patients were less impacted than DSA 1 patients, and we did not see a significant change in their probability of offer acceptance (compared to Set 1).

Set 3 (and its comparison with Set 1): In Set 3, we decrease the supply at DSA 3 such that the new s/d ratio in DSA 3 becomes 0.5 (from 0.7). The DSA 3 patients have a higher probability of offer acceptance than DSA 1 and 2 patients in lower-MELD categories (MELD 6-28).

Upon comparing with Set 1, we see that DSA 3 patients react by increasing their probability of offer acceptance (especially at MELD 6-32). DSA 1 and 2 patients also felt the effect, and they became more aggressive (than Set 1), especially at MELD 6-32.

Set 4 (and its comparison with Set 1): In Set 4, we increase the supply and demand volume at DSA 2 by 40%. The DSA 2 patients became more selective than DSA 1 patients at MELD 15-28 (and MELD 29-32 in the Share 35 policy but not in the Acuity Circles policy) due to an enlarged supply from where the patients could receive an offer.

Upon comparing with Set 1, we see that DSA 2 patients react by becoming more selective, especially at MELD 15-36 (except that MELD 33-34 did not see a significant effect in the Acuity Circles policy). DSA 1 and DSA 3 patients also became more selective (than Set 1), especially at MELD 29-36 and MELD 29-34, respectively. The selectiveness in the patient's behavior (compared to Set 1) is driven by the enlarged supply (even though demand also proportionally increased) from where the patients could receive an offer.

Set 5 (and its comparison with Set 1): In Set 5, we increase the supply and demand volume at DSA 3 by 40%. The DSA 3 patients are more selective than DSA 1 and 2 patients at MELD 15-34.

Upon comparing with Set 1, we see that DSA 3 patients react by becoming more selective, especially at MELD 15-36. DSA 1 and 2 patients also became more selective (than Set 1), especially at MELD 29-36. Again, the selectiveness in the patient's behavior (compared to Set 1) is driven by the enlarged supply (even though demand also proportionally increased) from where the patients could receive an offer.

To summarise, the main insights are: (1) When the s/d ratio differs between two DSAs, its impact (in terms of the probability of offer acceptance) is felt more in lower-MELD patients. The impact becomes attenuated at higher MELD scores due to the prioritization of higher-MELD patients through broader sharing (Share 35 and the Acuity Circles policy). If the s/d ratio decreases at a DSA, their patients react by becoming aggressive in organ acceptance behavior. (2) Increasing the supply and demand volume (keeping the s/d ratio the same) in a DSA leads to an enlarged supply from where the patients can receive an offer, which induces selective behavior. This behavioral change is not just limited to the DSA at which a change is made; it also has a spillover effect on other DSAs.

EC.10. Models for Benchmarking

In Table EC.6, we report the coefficients corresponding to various logistic regression models (RM1, RM2, and RM3) that we used for benchmarking. The dependent variable in all the models is the accept/decline decision.

In Figure EC.3(a), we plot the average probability of offer acceptance (calculated as a fraction of offers that were accepted) by MELD category, which we use as a reference. In Figure EC.3(b), (c), and (d), we plot the reduced-form models' predicted probabilities of offer acceptance. RM1 and RM2 do not capture the trend of the offer acceptance probability (with the MELD category), and the regime shift (from the Pre-Share 35 to Share 35 policy). RM3, which has more variables, is relatively better.

EC.11. Comparison of the Pre-Share 35 and Share 35 Policies on Geographic Equity Using Simulation

We use the simulation setup described in EC.8 to compare the Pre-Share 35 and Share 35 policies on a few geographic equity metrics. Referring to Figure 5, we see that not all regions benefit from introducing the Share 35 policy (compared to the Pre-Share 35 policy). For example, Region 11 becomes adversely impacted: the number of deaths and the amount of waiting time increased, and the number of transplants decreased. To gain more insights, we performed a simple correlation study (at the regional level) between the reduction in the number of deaths (normalized by the

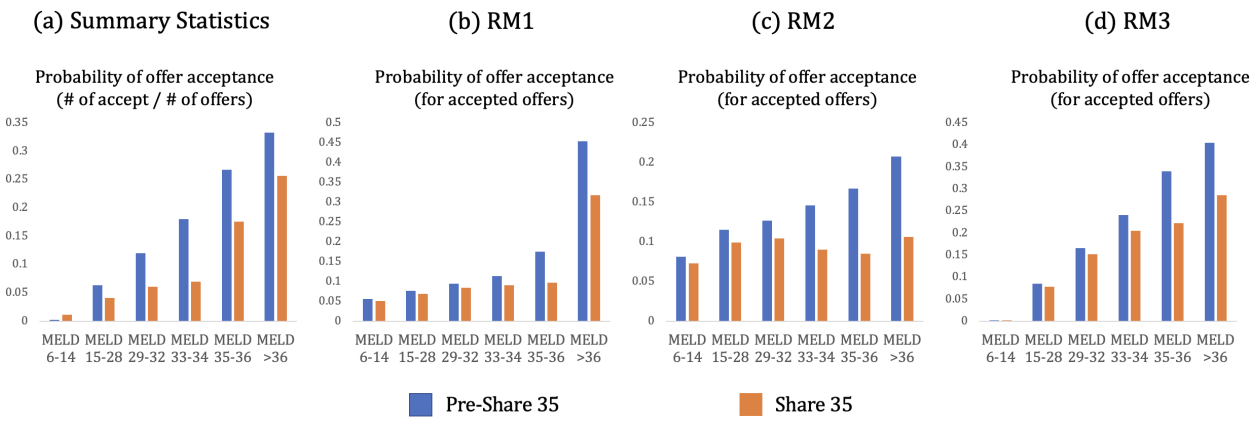

Figure EC.3 Out-of-sample comparison of reduced-form models.

waiting-list volume) and the s/d ratios (deceased donors in a region constitute the supply, and the total number of patients joining the waiting list in that region constitute the demand). We observed a strong negative correlation coefficient ($r = -0.91$; $P < 0.001$), suggesting that the benefit in terms of life savings due to the Share 35 policy is higher for regions with lower s/d ratios. This is reflective of the change brought due to the Share 35 policy that prioritized MELD $\geq$15 national patients before MELD <15 local or regional patients (see Table 2). A similar correlation study between the increase in the number of transplants (from the Pre-Share 35 to Share 35 policy) and the s/d ratios revealed a strong negative correlation coefficient ($r = -0.89$; $P < 0.001$). The reduction in the expected waiting period was also negatively correlated ($r = -0.93$; $P < 0.001$) with

Independent variable	Reduced-form Models		
	RM1	RM2	RM3
Intercept	-20.659***	-16***	-5.714***
Graft survival probability (GS)	19.322***	15.136***	-
MELD 15-28	-	-	3.287***
MELD 29-32	-	-	3.987***
MELD 33-34	-	-	4.419***
MELD 35-36	-	-	4.899***
MELD >36	-	-	5.2***
P(death|MELD)	80.745***	-	-
Wait time (in years)	-	-0.423***	-
Sharing type: Regional	-1.228***	-1.224***	-1.089***
Sharing type: National	-2.105***	-1.969***	-2.38***
Candidate age group: R2 (45-65 years)	0.433***	0.278***	0.182***
Candidate age group: R3 ($\geq$65 years)	0.546***	0.356***	0.085**
Candidate life support: Yes	0.962***	1.165***	-0.058
Candidate medical condition: H	1.079***	1.278***	0.549***
Candidate medical condition: ICU	1.735***	2.398***	0.625***
Log-likelihood	-57,861.72	-58,629.47	-53,815.62
No. of observations = 277,367			

***$p < 0.001$; **$p < 0.01$; *$p < 0.05$

Table EC.6 Regression estimates of the reduced-form models used for benchmarking.

Covariate	Graft survival	Patient survival without transplant
	Hazard ratio	Hazard ratio
MELD 6-14	1.13^{*}	0.45^{***}
MELD 29-32	0.91^{*}	3.63^{***}
MELD 33-34	0.75^{***}	4.49^{***}
MELD 35-36	0.92	5.97^{***}
MELD >36	1.04	11.24^{***}
Candidate age group: R1 (<45 years)	1.51^{***}	0.63^{***}
Candidate age group: R3 (≥65 years)	0.65^{***}	1.28^{***}
Candidate life support: Yes	1.09	2.67^{***}
Candidate medical condition: H	1.18^{***}	1.65^{***}
Candidate medical condition: ICU	1.09	2.07^{***}
Donor age group: (40 to 49 years)	1.35^{***}	-
Donor age group: (50 to 59 years)	1.58^{***}	-
Donor age group: (≥60 years)	1.78^{***}	-
Donor race: Other	1.08^{**}	-
Donor cause of death: Anoxia	0.84^{***}	-
Donor cause of death: CVA	1.10^{**}	-
Donor DCD: Yes	1.56^{***}	-
Sharing type: Regional	1.00	-
Sharing type: National	1.34^{***}	-

$^{***}p < 0.001$; $^{**}p < 0.01$; $^{*}p < 0.05$

Table EC.7 Survival model estimates.

the s/d ratios. Along these same lines, the increase in the expected offers was negatively correlated ($r = -0.68$; $P = 0.021$) with the s/d ratios.

EC.12. Survival Benefit due to a Transplant

We estimate the survival benefit due to a transplant as the difference between the probability of graft survival and the probability of a patient's survival without a transplant, both calculated at the end of one year. The baseline survival functions are estimated using the Kaplan-Meier curves. The estimated graft survival probability (at t=1 year) of the baseline is 0.98 (standard error = 0.05), and the patient's survival probability without a transplant of the baseline is 0.875 (standard error = 0.04). We use the Cox-proportional hazards model (Cox 1972) to estimate the hazard ratios (HR) associated with the organ and patient characteristics used in our simulation study. The estimates of the HRs are reported in Table EC.7.

EC.13. s/d Match Policy (Maximum Radius = 600 NM)

When we allow the maximum radius around the donor hospital to be 600 NM, the s/d ratio (at the TC level) ranges from 0.62 to 0.73. In Table EC.8, we compare the geographic equity metrics between the two s/d Match policies (maximum radius equals 500 NM versus 600 NM) using the simulation setup described in EC.8. Although we do not observe improvement in all the metrics, the expected number of deaths decreases from 459.9 (maximum radius = 500 NM) to 455.4 (maximum radius = 600 NM), and the expected number of transplants increases from 3,570.8 to 3,578.5.

Geographic equity metrics (normalized)	Standard deviation across the regions	
	s/d Match (500 NM)	s/d Match (600 NM)
Deaths	0.013	0.013
Transplants	0.028	0.034
Waiting (in months)	0.801	0.793
Offers	1.553	1.994

Table EC.8 Comparison of the standard deviation of various geographic equity measures between s/d Match policies.

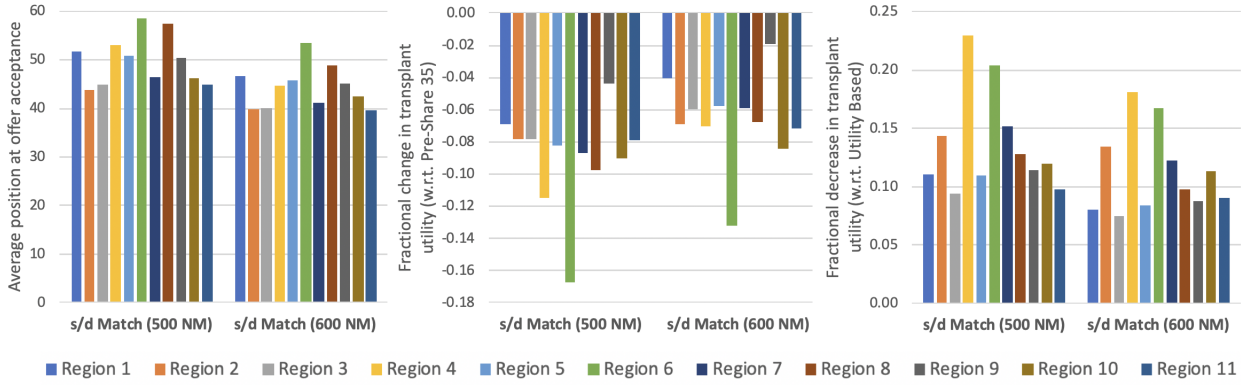

Figure EC.4 Comparison of the position at offer acceptance, fractional change in utility from the transplant (with respect to Pre-Share 35), and cost of fairness (with respect to Outcome-based) between the two s/d Match policies.

	s/d Match (500 NM)	s/d Match (600 NM)
Mean	360	337
1st quartile	52	60
Median	180	206
3rd quartile	417	427

Table EC.9 Comparison of travel distance (in NM) between the two s/d Match policies.

In Figure EC.4, we compare the efficiency metrics such as the position at offer acceptance, fractional change in the utility from the transplant (with respect to the Pre-Share 35 policy), and cost of fairness (with respect to the Outcome-based policy) between the two s/d Match policies. We see that the bigger radius policy results in greater efficiency. The average increase in a patient's survival probability due to a transplant is also slightly higher (0.185 versus 0.183) in the bigger radius s/d Match policy. Table EC.9 compares the distance traveled by the organ between the two s/d Match policies. While the mean distance is lower in the bigger radius policy, the other measures are marginally higher. In conclusion, if broader sharing is done right by matching supply and demand, it results in greater equity with minimal impact on the efficiency metrics!